This paper has been published under the following reference: Ahmadi, E., Caprani, C., Živanović, S., Evans, N. and Heidarpour, A. (2018) A framework for quantification of human-structure interaction in vertical direction. *Journal of Sound and Vibration*, Vol. 432, pp. 351-372. (https://doi.org/10.1016/j.jsv.2018.06.054)

A Framework for Quantification of Human-Structure Interaction in Vertical Direction

Ehsan Ahmadi[1], Colin Caprani[1]*, Stana Živanović[2], Neil Evans[2], Amin Heidarpour[1]
[1] Dept. of Civil Engineering, Monash University, Australia
[2] School of Engineering, University of Warwick, UK
* Corresponding Author

Abstract

In lightweight structures, there is increasing evidence of the existence of interaction between pedestrians and structures, now commonly termed pedestrian-structure interaction. The presence of a walker can alter the dynamic characteristics of the human-structure system compared with those inherent to the empty structure. Conversely, the response of the structure can influence human behaviour and hence alter the applied loading. In the past, most effort on determining the imparted footfall-induced vertical forces to the walking surface has been conducted using rigid, non-flexible surfaces such as treadmills. However, should the walking surface be vibrating, the characteristics of human walking could change to maximize comfort. Knowledge of pedestrian-structure interaction effects is currently limited, and it is often quoted as a reason for our inability to predict vibration response accurately. This work aims to quantify the magnitude of human-structure interaction through a experimental-numerical programme on a full-scale lively footbridge. An insole pressure measurement system was used to measure the human-imparted force on both rigid and lively surfaces. Test subjects, walking at different pacing frequencies, took part in the test programme to infer the existence of the two forms of human-structure interaction. Parametric statistical hypothesis testing provides evidence on the existence of human-structure interaction. In addition, a non-parametric test (Monte Carlo simulation) is employed to quantify the effects of numerical model error on the identified human-structure interaction forms. It is concluded that human-structure interaction is an

important phenomenon that should be considered in the design and assessment of vibration-sensitive structures.

Keywords

Human-structure interaction; footbridge vibration; experiment; in-sole sensors

1. Introduction

Many newly built structures have light weight, low damping, and low stiffness, and they may not satisfy vibration serviceability criteria when occupied and dynamically excited by humans [1]. Observed problems have been caused typically by human occupants performing normal activities such as walking, running, jumping, bouncing/bobbing, and dancing. Vibration beyond the human comfort range will influence human comfort and so is a key consideration for designers. Human presence can affect the dynamic characteristics of the coupled human-structure system during motion, named here as Human-to-Structure Interaction (H2SI). On the other hand, the vibrating structure may change the human activity force pattern, and this potential phenomenon is named here as a Structure-to-Human Interaction (S2HI) (Figure 1). These postulated mutual effects between human and structure are collectively referred to as human-structure interaction (HSI). Since for this work we consider only single human loading situations, we do not consider human-to-human interaction which can take place in crowds. The H2SI and S2HI effects are usually considered mutually exclusive [2], meaning that HSI is often modelled through a change in the dynamic properties of the system only or a change in walking force only. In this study, they are assumed to be mutually independent, isolated and examined individually using a novel experimental-numerical programme while both types occur simultaneously.

This paper has been published under the following reference: Ahmadi, E., Caprani, C., Živanović, S., Evans, N. and Heidarpour, A. (2018) A framework for quantification of human-structure interaction in vertical direction. *Journal of Sound and Vibration*, Vol. 432, pp. 351-372. (https://doi.org/10.1016/j.jsv.2018.06.054)

The focus of this study is on human walking and the resulting vibration. To assess the vibration response of structures susceptible to human walking, accurate estimation of human force, dynamic characteristics of the structure, and human-structure interaction are required (Figure 1). As a novel aspect of this work, human walking force was measured using TekScan F-scan in-shoe plantar pressure sensors intended for medical applications. The plantar pressure force gives a reliable measurement of the vertical walking force [3], [4]. Further, the mass, damping, and stiffness of the structure were obtained using system identification methods. The most challenging part of the study of human-structure interaction is to identify and quantify the postulated forms of HSI separately. This study proposes an experimental framework to address this challenge. It relies on acquiring sufficiently accurate measurements of the human force, structure dynamics, and comparison of data recorded on rigid and flexible surfaces. The two postulated forms of HSI will be described in more detail in the next two sections.

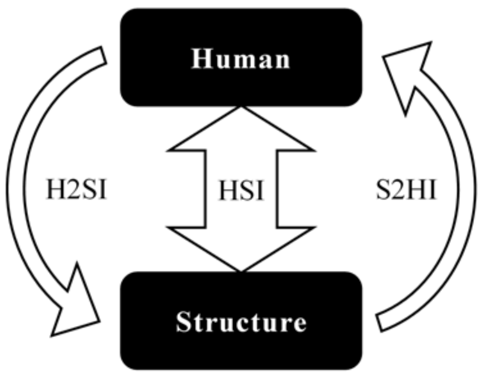

Figure 1 Interactions between humans and the structure in the human-structure system are collectively called Human-Structure Interaction (HSI), but are considered separately here as Human-to-Structure Interaction (H2SI) and Structure-to-Human Interaction (S2HI).

The human body is a sensitive vibration receiver characterized by an innate ability to adapt quickly to almost any type and level of vibration which normally occurs in nature [5]. This effective self-adapting mechanism triggers pedestrians to change their walking behaviour [6]. In turn, it leads to walking force patterns that can be different to those measured on non-vibrating rigid surfaces [7].

There have been numerous attempts to measure or model pedestrian-induced forces, referred to as ground reaction forces (GRFs); see for example [8], [9], [10], [11], [12], [13], [14]. Past GRF measurement facilities typically comprised equipment for direct force measurements, such as a force plate [15], or an instrumented treadmill usually mounted on rigid laboratory floors ([16], [17], [18]). However, GRFs could differ when walking on vibrating surface. For example, Ohlsson [19] found that the vertical force measured on a flexible timber floor is different from that measured on a rigid base. Pavic et al. [20] pointed out that the force induced by jumping on a flexible concrete beam was lower than that on a force plate. Van Nimmen et al. [21] and Bocian et al. [22] indirectly reconstructed vertical walking force on bridge surfaces from inertial motion tracking and a single point inertial measurement respectively. To the authors' knowledge, Dang and Zivanovic [23] is the only experimental work on direct measurement of walking GRFs on lively structures in the vertical direction. The results showed a drop in the first dynamic load factor of the walking force due to the bridge vibration at the resonance. However, test subjects walked on-the-spot on a treadmill for this study.

Humans add mass, stiffness, and damping to the coupled human-structure system. The influence of passive humans on the dynamic properties of the structure they occupy (i.e. modal mass, damping, and stiffness) have been well-documented in the literature [24], [2], [25], [26]. For example, Ohlsson [19] found that a walking pedestrian can increase the HSI system's frequency and damping, while Willford [27] also reported a change in the system's damping due to moving crowd in the vertical direction. Zivanovic et al. [28] and Van Nimmen et al. [29] identified modal properties of the HSI system and showed that the presence of humans on the structure, either in standing or walking form, will increase the damping of the system compared to the empty structure. Zivanovic et al. [30] revealed that crowd effects can be also modelled as an increase in the damping of the system, in some cases more than two times greater than the damping ratio for the empty bridge, and Caprani et al. [31] did so to account for crowd damping effects. Kasperski [32] also concluded that a walking pedestrian can induce additional damping by using discrete Fourier transform of the acceleration time history response of the bridge. However, these existing effects are not incorporated into design codes and guidelines such as OHBDC [33], U.K. National Annex to Eurocode 1 (British Standards Institution 2008) [34], ISO-10137 [35], Eurocode 5 [36], Setra [37], and HIVOSS [38] as they model humans as a moving force only. Interestingly, the U.K. National Annex to Eurocode 1 does acknowledge that H2SI effects exist, but does not offer guidance on their inclusion, underlining the need to quantify the H2SI effect on vibration.

The review above has shown that quantification of human-structure interaction is a crucial part of vibration response estimation and that there is some evidence of the two postulated forms of HSI in the literature. However, these HSI forms are not fully experimentally quantified, which is an essential step towards the development of design/assessment guidelines that can consider HSI. This work experimentally investigates the existence of the two postulated HSI forms by isolating their influence on the vibration response. To this end, a novel experimental-numerical programme is adopted. The human-imparted forces to both flexible (i.e. footbridge) and rigid surfaces are measured. These are then used to simulate the vibration response. The simulated vibration response from walking force measured on the rigid surface represents state-of-the-art practice. The vibration response of the footbridge is also directly measured. Comparison of dynamic load factors of the forces on the bridge surface with those of rigid surface should reveal any walking pattern change due to HSI (S2HI). Another comparison for simulated vibration responses due to the rigid and bridge surface walking forces discloses the effect of S2HI on the vibration response. Comparing the simulated bridge vibration response and the measured vibration response gives a good insight into the effects of HSI on the changes in

This paper has been published under the following reference: Ahmadi, E., Caprani, C., Živanović, S., Evans, N. and Heidarpour, A. (2018) A framework for quantification of human-structure interaction in vertical direction. *Journal of Sound and Vibration*, Vol. 432, pp. 351-372. (https://doi.org/10.1016/j.jsv.2018.06.054)

system dynamic characteristics (H2SI). A parametric statistical hypothesis test is then used to show the generality of the results for a large number of walking trial scenarios. Finally, a non-parametric test (Monte Carlo simulation) is conducted to determine the influence of model errors on the two postulated forms of HSI. This experimental-numerical approach is next described in detail.

2. Experimental Procedure

2.1 Experimental-numerical programme

Figure 2 schematically illustrates the experimental-numerical programme design to investigate HSI. Two types of measurement are taken: (1) GRFs from walking on a rigid surface (RS), G_{RS} (part (a) in Figure 2); (2) GRFs from walking on a vibrating bridge surface (BS), G_{BS} (part (b)), while the vibration response of the bridge, R_M (part (f)), is concurrently measured. Subsequent to these physical measurements, vibration responses to the measured RS and BS GRFs are simulated using a system model (part (c)), namely a modal model of the bridge and a moving force (MF) model of the pedestrian. These were denoted R_{RS} (part (d)), and R_{BS} (part (e)), respectively.

This paper has been published under the following reference: Ahmadi, E., Caprani, C., Živanović, S., Evans, N. and Heidarpour, A. (2018) A framework for quantification of human-structure interaction in vertical direction. *Journal of Sound and Vibration*, Vol. 432, pp. 351-372. (https://doi.org/10.1016/j.jsv.2018.06.054)

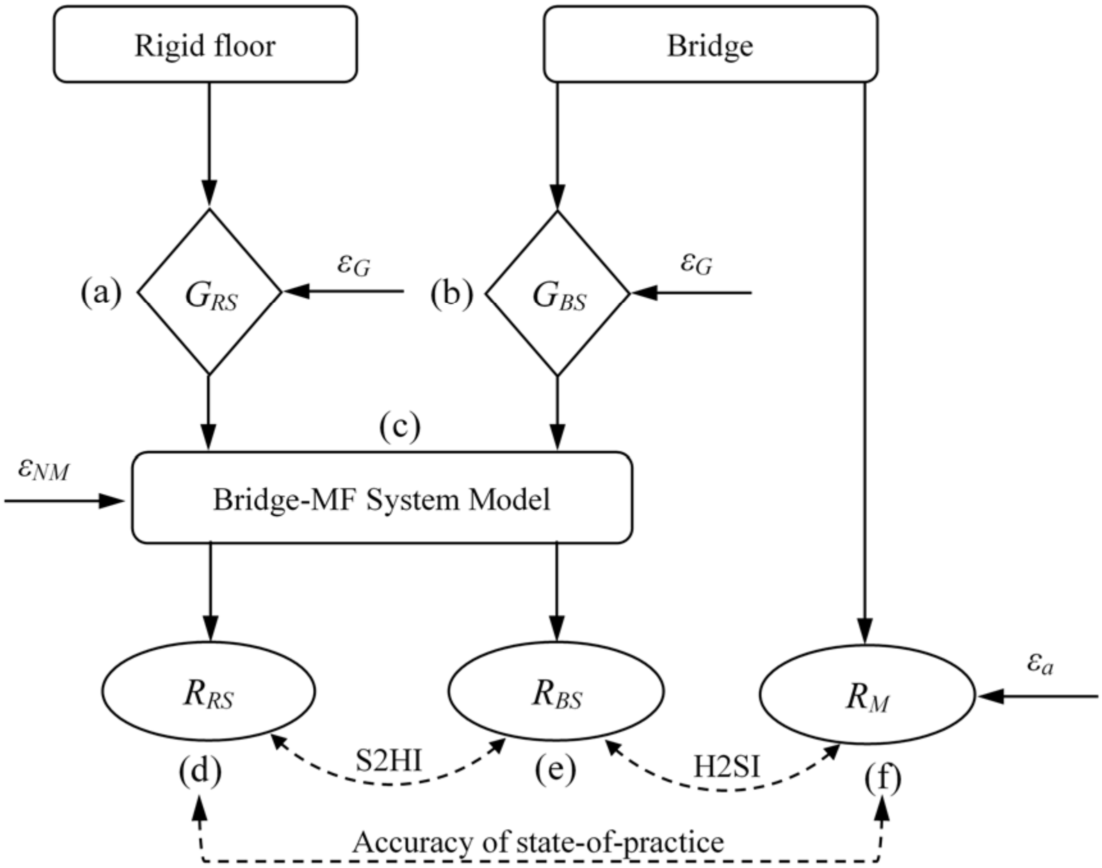

Figure 2 A schematic overview of the experimental-numerical programme, including an assessment of the accuracy of typical current practice using a moving force approach.

In this study, a difference between the vibration responses R_{RS} (part (d)) and R_{BS} (part (e)) of the analytical model is considered as evidence of the influence of the vibrating bridge surface on the walker-induced force (S2HI) (part (a) versus part (b)). Going a step farther, comparing the simulated vibration response, R_{BS} , to those measured from the bridge, R_M , yields the accuracy of the coupled bridge-MF system model (part (c)) itself. Here, there are two potential errors to the system model: (1) the accuracy of the bridge model, and (2) the accuracy of MF model due to H2SI. A reliable system identification method and using amplitude-dependent frequency and damping of the bridge can significantly increase the accuracy of the bridge model and reduce the first source of error in the system model to a very small amount. Consequently, any difference between R_{BS} and R_M is because the MF model is unable to insert human effects into the numerical model, H2SI. Further, comparison of R_{RS} and R_M implies the accuracy of state-of-the-art design practice as the MF model and rigid surface force are used to estimate the actual bridge response R_M.

The influence of errors in various measurements, ε, is also considered. The system numerical model error, ε_{NM}, and measurement errors, ε_G and ε_a will be discussed later. Monte Carlo simulations are performed to evaluate the influence of these errors (which are difficult to measure) on the HSI quantifications.

2.2 Walking trials

All tests were carried out on the Warwick Footbridge – a steel-concrete composite laboratory footbridge at the University of Warwick, UK, shown in Figure 3. The bridge is a unique laboratory structure purpose-built with a natural frequency in the vertical direction that can be matched by pacing rate, making it an ideal facility for studying HSI. The simply-supported span length of the bridge is adjustable, but was kept constant throughout the tests at 16.2 m. The bridge is 2 m wide, with a clear walkway track down the centre. The bridge mass is approximately 16500 kg, and the modal mass of the first bending mode is 7614 kg with natural frequency of about 2.43 Hz [39]. As a unique facility, it has already been used considerably for the study of human-induced vibration [23].

This paper has been published under the following reference: Ahmadi, E., Caprani, C., Živanović, S., Evans, N. and Heidarpour, A. (2018) A framework for quantification of human-structure interaction in vertical direction. *Journal of Sound and Vibration*, Vol. 432, pp. 351-372. (https://doi.org/10.1016/j.jsv.2018.06.054)

Figure 3 The Warwick footbridge.

The tests comprised of walking at 2.4 Hz to excite the resonance by the first forcing harmonic, walking at 1.2 Hz to excite the resonance by the second harmonic, and walking at 2.1 Hz to expose the test subject to the beating vibration response. 2.4 Hz covers upper bound of normal pacing frequency range of a pedestrian (1.6-2.4 Hz). In this paper, the pacing-to-bridge frequency ratio ($\beta = f_p/f_b$) is used, and so $\beta \in \{0.5, 0.87, 1.0\}$.

Five test subjects (4 male, 1 female), weighing from 543 N to 1117 N participated in the experiments. The test subject-to-bridge mass ratio, $\mu_m = m_p/m_b$ ranged from 0.33-0.7% and it will be used later to discuss the results for each test subject. For each trial, test subjects walked a circuit including a rigid surface (RS) and bridge surface (BS) as shown in Figure 4. On both surfaces, the walking length was the same (16.2 m). After a sound signal, test subjects started walking. A metronome was used during each trial so that test subjects targeted the desired pacing frequency. Each walking trial was repeated until five successful trials were recorded. It should be stated that all trials were carried out in accordance with The Code of Ethics of the World Medical Association (Declaration of Helsinki).

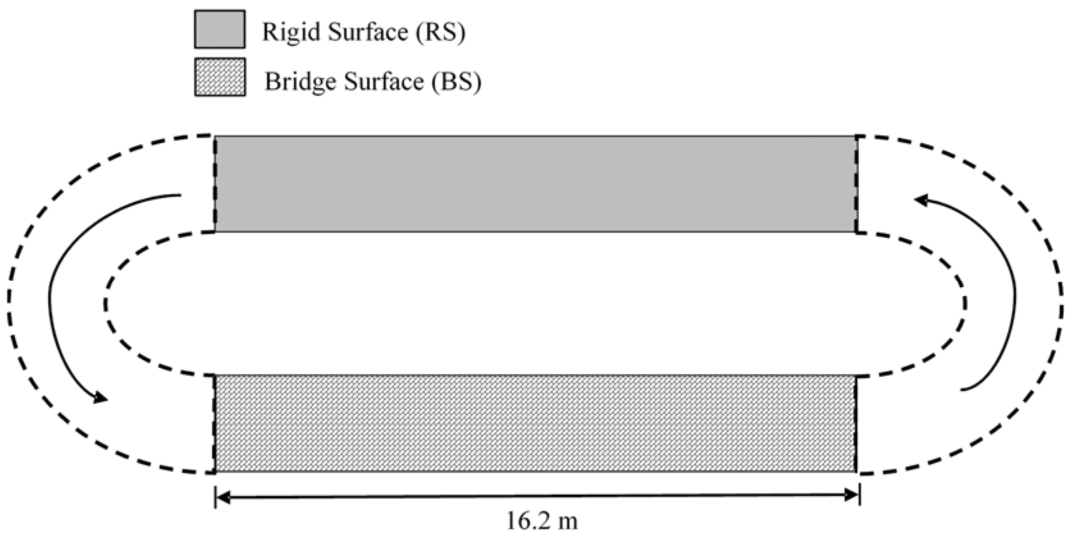

Figure 4 Schematic plan of the walking trials path.

2.3 Data acquisition

To record input forces and output accelerations data, a test set-up was designed as shown in Figure 5. The bridge vibration was measured using two Honeywell QA750 accelerometers, placed at mid-span and quarter-span points. The accelerometer signals were recorded using Quattro data acquisition (DAQ) unit by Data Physics (see Figure 5). The TekScan equipment was used for collecting the GRFs of the rigid and bridge surfaces throughout the walking trials. A TekScan trigger transmitter and two TekScan trigger receivers were used to synchronize recordings remotely. One trigger receiver was connected to the data recorder of the TekScan system, and the other one was attached to the Quattro DAQ. Note that unusually, the trigger was not used to trigger recording, rather its voltage output was recorded to identify the time window when the test subject was occupying the bridge. Thus, when the test subject was visually observed to be at the end of the footbridge a further trigger signal was given, changing the trigger output voltage, though data continued to be collected (e.g. free-vibration). Figure 6 shows a typical trigger voltage signal for the test subject of μ_m = 0.6 % and trial No. 5 with

This paper has been published under the following reference: Ahmadi, E., Caprani, C., Živanović, S., Evans, N. and Heidarpour, A. (2018) A framework for quantification of human-structure interaction in vertical direction. *Journal of Sound and Vibration*, Vol. 432, pp. 351-372. (https://doi.org/10.1016/j.jsv.2018.06.054)

frequency ratio of 1. This specific test subject, trial, and frequency ratio will be used as a running example through the paper.

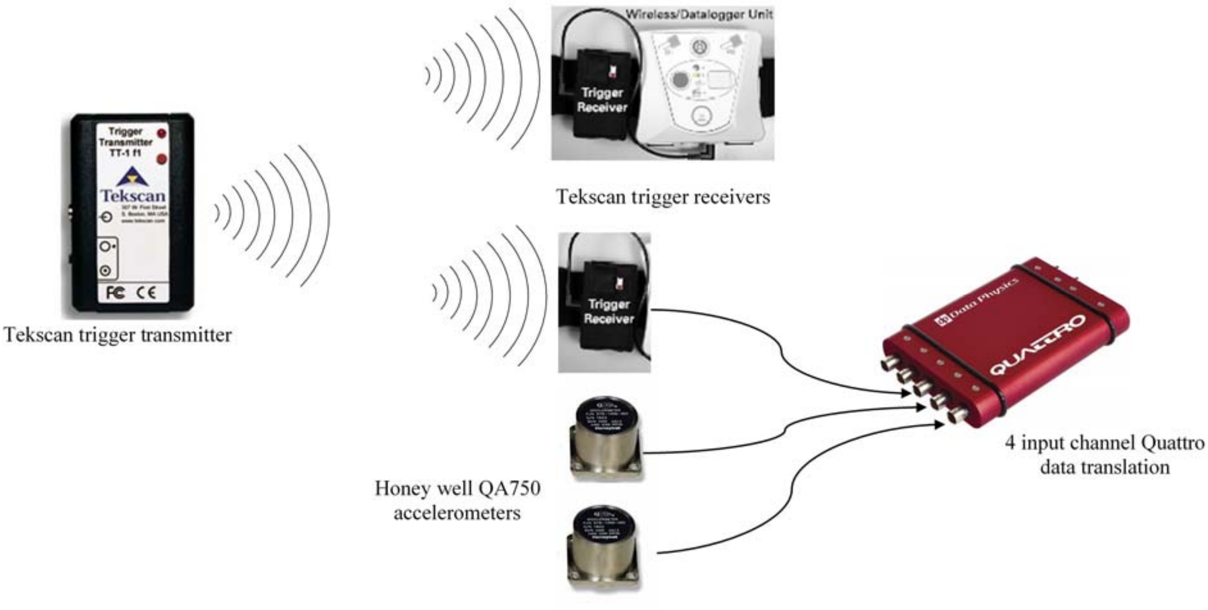

Figure 5 Test set-up for data acquisition.

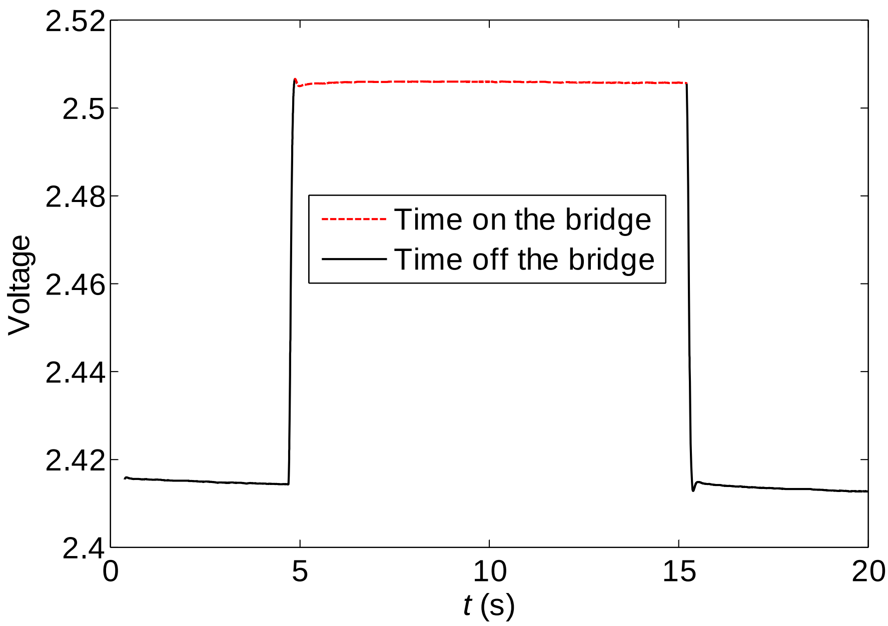

Figure 6 Voltage signal for time on and off the bridge for the example test subject, μ_m = 0.6 % and trial No. 5 with frequency ratio of 1.

3. Experimental Results

3.1 Footbridge frequency and damping

Free decay vibration measurements were made to investigate dynamic characteristics of the footbridge. It was found that the bridge frequency, f_b, and damping, ξ_b, are amplitude-dependent. To determine the bridge damping, an exponential decay curve is fitted (using least-squares) to a moving window of five peaks (Figure 7a). It was found that the damping ratio increases with an increase in the vibration amplitude, a_p, as shown in Figure 7b. This is a common feature of real structures because there are more sources and increased energy dissipation at higher vibration amplitudes. Nevertheless, the maximum damping ratio of about 0.5% is still quite low, ensuring lively behaviour. The natural frequency was found to decrease slightly with an increase in the vibration amplitude (Figure 7c). This is also typical behaviour in civil engineering structures. Finally, data points were fitted to model the relationship between damping and vibration amplitude, as well as frequency and vibration amplitude (Figures 7b and 7c). These relationships are used in the numerical simulations.

This paper has been published under the following reference: Ahmadi, E., Caprani, C., Živanović, S., Evans, N. and Heidarpour, A. (2018) A framework for quantification of human-structure interaction in vertical direction. *Journal of Sound and Vibration*, Vol. 432, pp. 351-372. (https://doi.org/10.1016/j.jsv.2018.06.054)

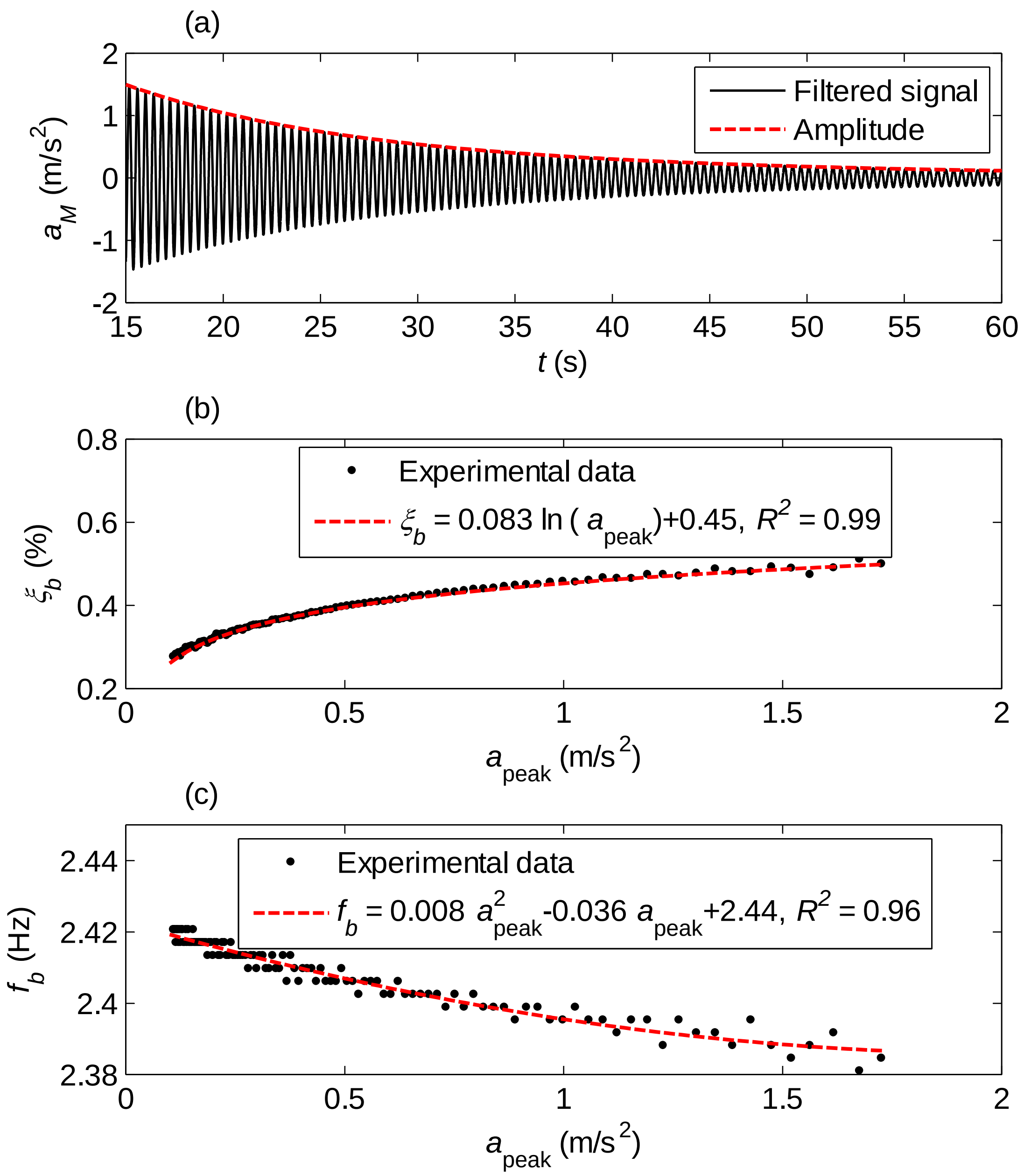

Figure 7 (a) free decay vibration time history and its amplitude for the bridge (a low-pass 4th order Butterworth filter with cut-off frequency, 10 Hz, was used); (b) amplitude-dependent bridge damping results and model (c) amplitude-dependent bridge frequency results and model.

3.2 Measured vibration responses

The mid-span acceleration response of the bridge to a walking trial, in which a test subject walked at 2.4 Hz (hereafter referred to as the exemplary test subject and trial), is illustrated in Figure 8a. Noise in the measured signal was removed using a low-pass 4th order Butterworth

This paper has been published under the following reference: Ahmadi, E., Caprani, C., Živanović, S., Evans, N. and Heidarpour, A. (2018) A framework for quantification of human-structure interaction in vertical direction. *Journal of Sound and Vibration*, Vol. 432, pp. 351-372. (https://doi.org/10.1016/j.jsv.2018.06.054)

filter with cut-off frequency of 10 Hz. The cut-off frequency of 10 Hz is more than four times the bridge fundamental frequency and so the results will not be influenced by the filter roll-off. The corresponding power spectrum density (PSD) of the acceleration signal, shown in Figure 8b, reveals that most of the response energy is concentrated at the first vibration mode of the bridge.

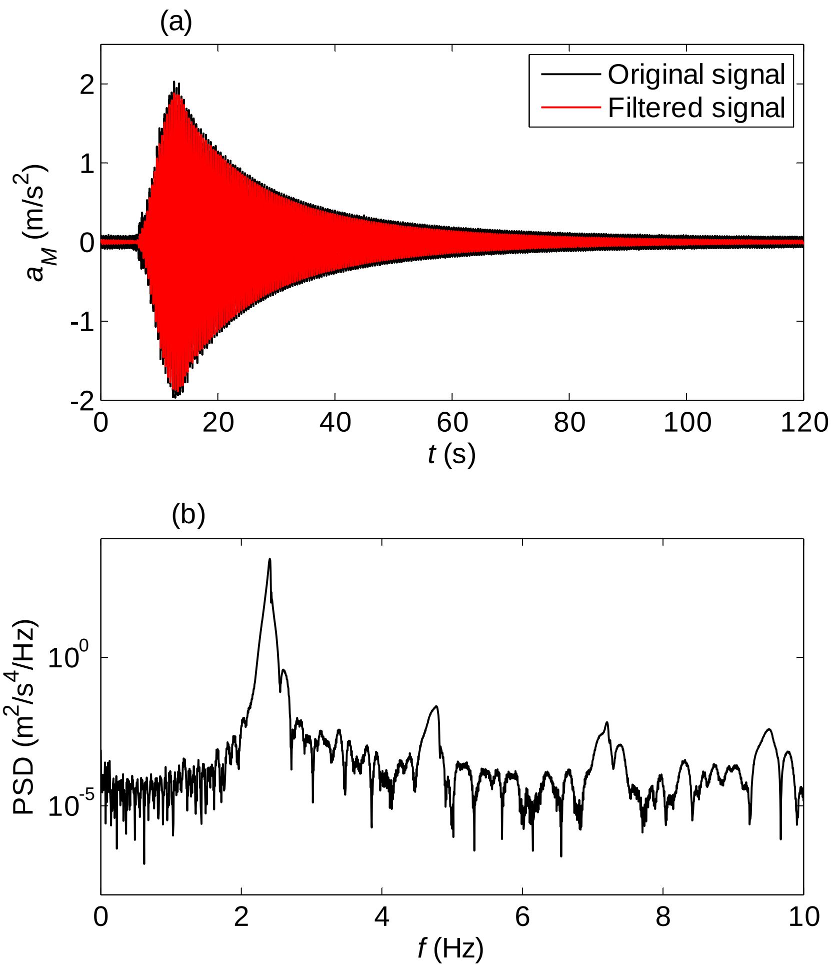

Figure 8 (a) bridge mid-span acceleration response (b) its corresponding power spectral density (PSD) for the exemplary test subject (trial of Figure 6).

The maximum response for each acceleration signal is selected as the response metric. Table 1 summarizes the maximum acceleration response, a_{max}, for each test subject, pacing frequency, and trial. The maximum accelerations from Table 1 can be compared with the limits in the

This paper has been published under the following reference: Ahmadi, E., Caprani, C., Živanović, S., Evans, N. and Heidarpour, A. (2018) A framework for quantification of human-structure interaction in vertical direction. *Journal of Sound and Vibration*, Vol. 432, pp. 351-372. (https://doi.org/10.1016/j.jsv.2018.06.054)

Setra guideline [37], shown in Table 2. In many cases, the footbridge provides either "minimum" or "unacceptable vibration" comfort level to the test subject, demonstrating the liveliness of the structure.

Table 1. Maximum measured acceleration response (a_{max}, m/s^2).

Test Subject	Mass Ratio, μ_m (%)	Frequency Ratio, β	Trial No. 1	2	3	4	5	Mean
1	0.33	0.50	0.22	0.22	0.21	0.22	0.25	0.22
		0.87	0.17	0.21	0.20	0.15	0.19	0.18
		1.00	1.32	1.40	1.28	1.24	1.33	1.31
2	0.40	0.50	0.19	0.17	0.17	0.18	0.20	0.18
		0.87	0.19	0.24	0.17	0.16	0.20	0.19
		1.00	1.26	1.43	1.32	1.28	1.26	1.31
3	0.50	0.50	0.16	0.25	0.15	0.20	0.18	0.19
		0.87	0.35	0.20	0.22	0.22	0.22	0.24
		1.00	1.33	1.05	1.43	1.32	1.43	1.31
4	0.60	0.50	0.25	0.23	0.25	0.37	0.30	0.28
		0.87	0.21	0.28	0.28	0.27	0.24	0.26
		1.00	1.34	1.83	1.82	1.84	1.87	1.74
5	0.70	0.50	0.49	0.53	0.46	0.62	0.57	0.53
		0.87	0.29	0.35	0.54	0.28	0.37	0.37
		1.00	2.48	2.38	2.63	2.50	2.53	2.51

Table 2. Comfort levels and acceleration ranges (from [7]).

Comfort Level	Degree of comfort	Vertical acceleration limits (m/s^2)
CL 1	Maximum	< 0.5
CL 2	Medium	0.5 – 1.0
CL 3	Minimum	1.0 – 2.5
CL 4	Unacceptable vibration	> 2.5

3.3 GRFs signal acquisition and processing

To measure the GRFs on both the rigid and flexible surfaces during walking, a novel experimental approach was employed. TekScan F-Scan in-shoe plantar pressure sensors developed for medical applications were used [3], [40], [41]. The measured pressure profiles were integrated to determine force time histories for each foot allowing detailed gait analysis. TekScan F-scan in-shoe sensors, pressure distribution, and bridge surface force signals, G_{BS}, of left and right feet for the exemplary test subject are shown in Figure 9.

The sensors are made up of 960 individual pressure sensing capacitor cells, which are referred to as sensels. The sensels are arranged in rows and columns on each sensor. The 8-bit output of each sensel is divided into $2^8 = 256$ increments, and displayed as a value (Raw Sum), in the range of 0 to 255 by the F-scan software. If all sensels reach a raw count of 255, the corresponding pressure is called saturation pressure. Although raw sum display shows relative force differences on the sensor, this data is more meaningful if the force is calibrated to give engineering measurement units. Obviously, proper calibration of the sensors is critical to obtaining accurate force readings. When a test subject walks, there must be sufficient raw output generated from the sensor so the calibration is accurate. It is also necessary to zero the sensor output. Indeed, when one foot is supporting the body weight during walking, the other foot is up in the air and its force should be zero. However, because the foot sensors are pre-tensioned to the sole of the foot by shoe-lacing, the output of sensors is not zero when foot is not touching the ground (Figure 9). Hence, it is necessary to zero the force output for each trial during a swing phase of walking.

This paper has been published under the following reference: Ahmadi, E., Caprani, C., Živanović, S., Evans, N. and Heidarpour, A. (2018) A framework for quantification of human-structure interaction in vertical direction. *Journal of Sound and Vibration*, Vol. 432, pp. 351-372. (https://doi.org/10.1016/j.jsv.2018.06.054)

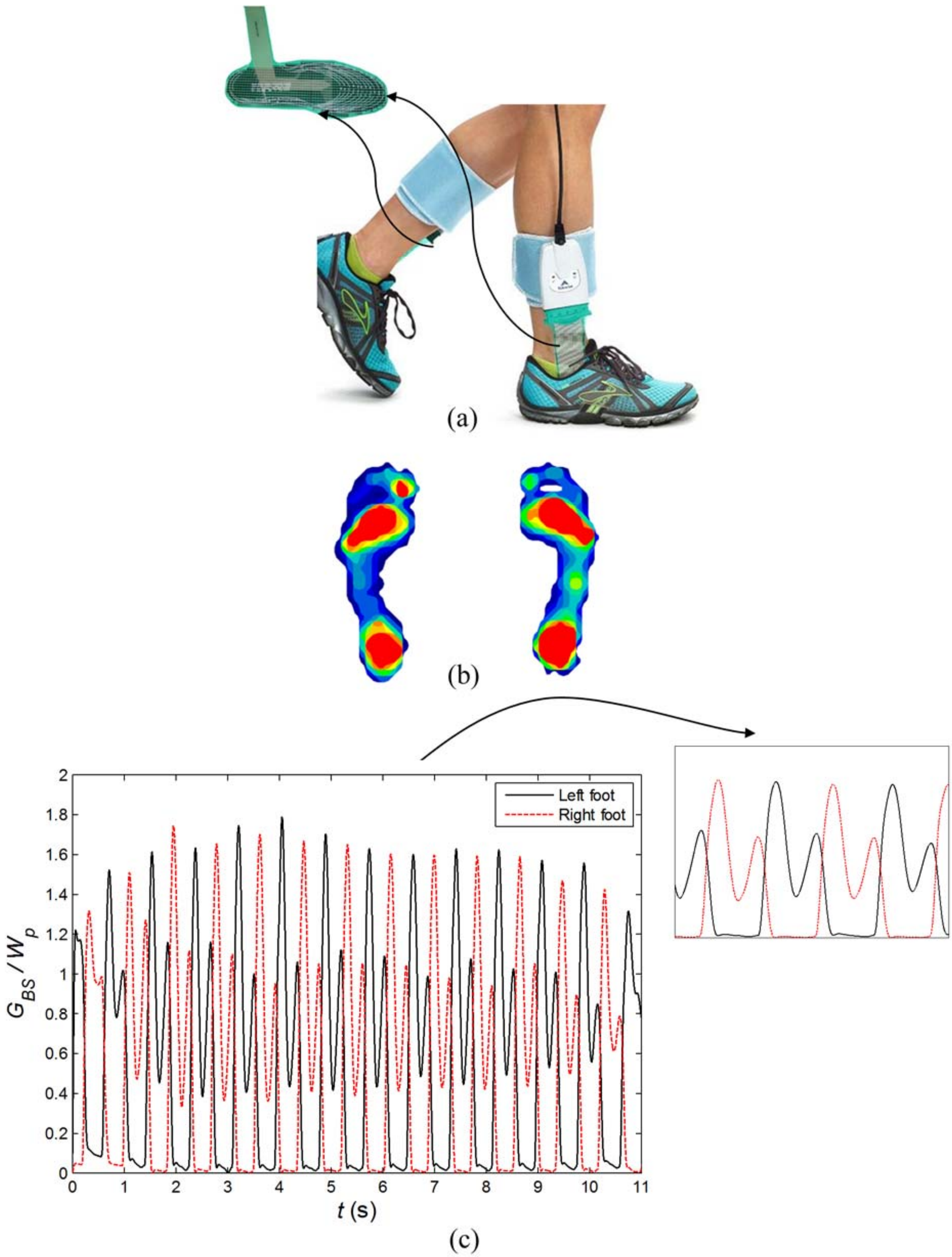

Figure 9 TekScan F-scan in-shoe sensors: (a) as worn by subject (image taken from [42] and used with permission of Tekscan company), (b) output pressure distribution under a standing subject, and (c) bridge surface force signals of left and right feet for the exemplary test subject.

The TekScan software supports five methods for calibrating sensors: point calibration, step calibration, walk calibration, frame calibration, and two-point calibration. All of these methods

This paper has been published under the following reference: Ahmadi, E., Caprani, C., Živanović, S., Evans, N. and Heidarpour, A. (2018) A framework for quantification of human-structure interaction in vertical direction. *Journal of Sound and Vibration*, Vol. 432, pp. 351-372. (https://doi.org/10.1016/j.jsv.2018.06.054)

were considered for accuracy using a force plate as a benchmark before the main trials were conducted. A walk calibration was found to give higher accuracy in the regions of interest compared to step calibration using the same factors. Of most interest, step calibration and walk calibration use the test subject's weight to adjust the calibration factor. As seen in Figure 10, the walk calibration estimates walking force with an accuracy considered reasonable for this work. It gives good result for the heel-strike phase while it underestimates the pedestrian force somewhat for toe-off phase. Calibration of the sensor is carried out for each trial using the test subject weight and rigid surface force time history. Thus, each trial conducted has its own calibration factor.

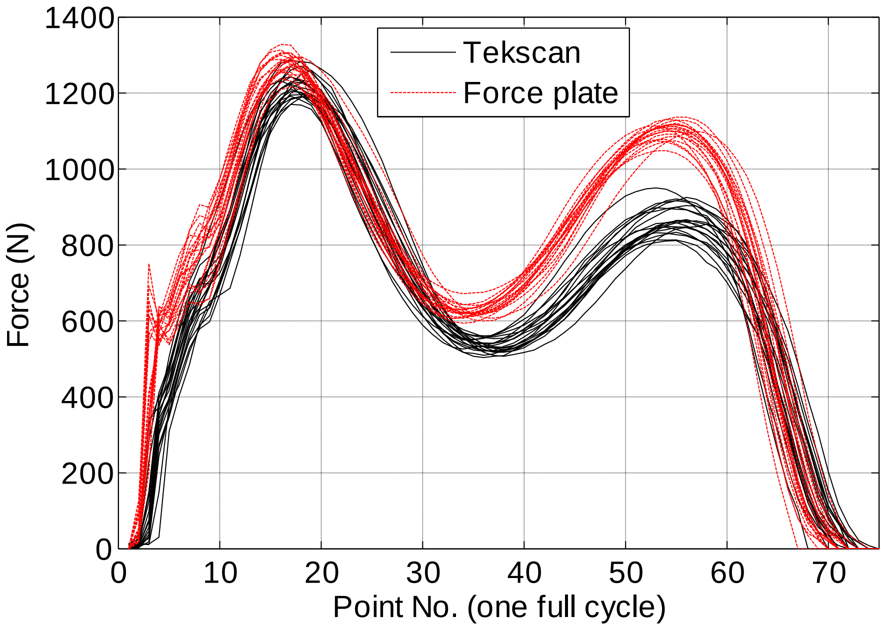

Figure 10 TekScan (walk calibration) and force plate results for pacing frequency of 2 Hz, 20 trials, left foot, and one full cycle.

There is one further aspect of the TekScan sensors that benefits from giving each trial its own calibration factor. Due to degradation of the sensor, drift of the sensor output can occur over time. Additionally, the sensors can deteriorate so that rows or columns of the sensels no longer export forces. Saturation pressure (described above) is closely related to the calibration factor.

This paper has been published under the following reference: Ahmadi, E., Caprani, C., Živanović, S., Evans, N. and Heidarpour, A. (2018) A framework for quantification of human-structure interaction in vertical direction. *Journal of Sound and Vibration*, Vol. 432, pp. 351-372. (https://doi.org/10.1016/j.jsv.2018.06.054)

Therefore, if some sensors damage during walking, the saturation pressure will change and so this was tracked throughout the trials. Figure 11 shows a sample of saturation pressure record for one test subject for the pacing frequency of 2.4 Hz. It can be seen that sensor degradation is small because the saturation pressures over a period of about 1.5 hours remain reasonably consistent.

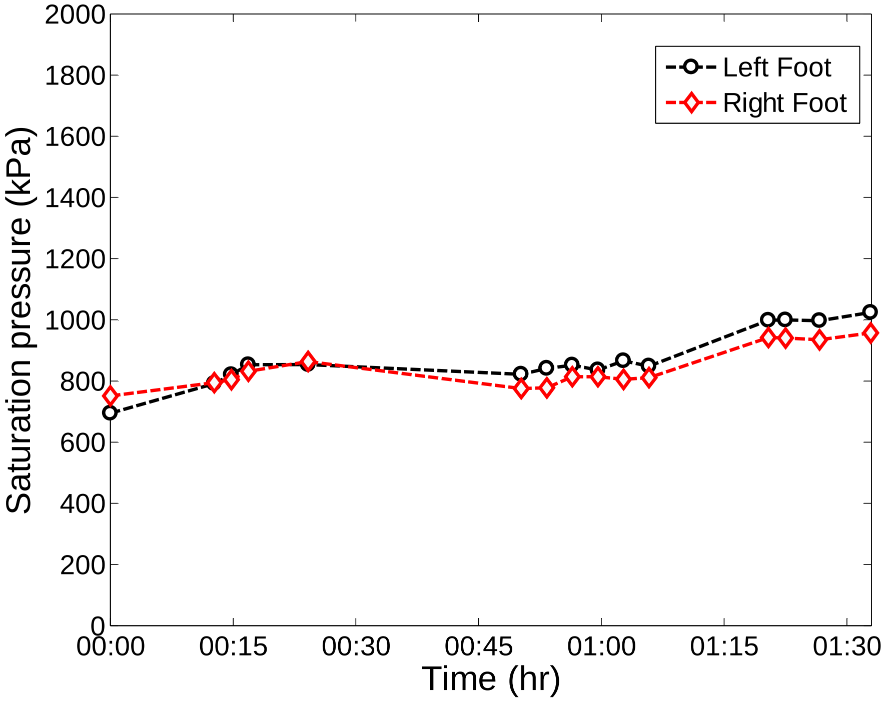

Figure 11 Saturation pressure vs. time (hour) for one test subject and pacing frequency of 2.4 Hz.

4. Data Analysis

4.1 Dynamic load factors

Walking forces are commonly described using a Fourier series [24]:

$$G(t) = W_p \sum_{k=0}^{r} \mathrm{DLF}_k \cos\left(2\pi k f_p t + \varphi_k\right) \qquad (1)$$

where $W_p = m_p g$; m_p is the pedestrian mass; g is the acceleration due to gravity; f_p is the pacing frequency; and DLF_k is the dynamic load factor for the kth harmonic. The phase angle of the kth harmonic is denoted by φ_k , and r represents total number of harmonics considered. In this representation, the harmonic $k = 0$ corresponds to the static pedestrian weight, and so $\varphi_0 = 0$ to give $\text{DLF}_0 = 1$. To calculate the DLFs from the GRF measurements, the start and end of the recorded walking force signals are trimmed such that a signal consists of some even number of full steps achieved. Then, the DC component is subtracted from the signal and then the signal is windowed using a Hann window to suppress leakage. The signal is zero-padded afterwards and transformed into the frequency domain using the Fast Fourier Transform (FFT). The signal amplitude in the frequency domain is corrected for the side-lobe loss due to using Hann window [43]. Figure 12 shows all steps to determine dynamic load factor for the exemplary test subject, highlighting the first four DLFs. Consistent with the literature, the pedestrian force is not perfectly periodic; in fact, it is a narrow band signal with some of its energy spread to adjacent frequencies [44], [45]. Phase angles are also found to be more or less uniformly distributed from 0 to π radians.

This paper has been published under the following reference: Ahmadi, E., Caprani, C., Živanović, S., Evans, N. and Heidarpour, A. (2018) A framework for quantification of human-structure interaction in vertical direction. *Journal of Sound and Vibration*, Vol. 432, pp. 351-372. (https://doi.org/10.1016/j.jsv.2018.06.054)

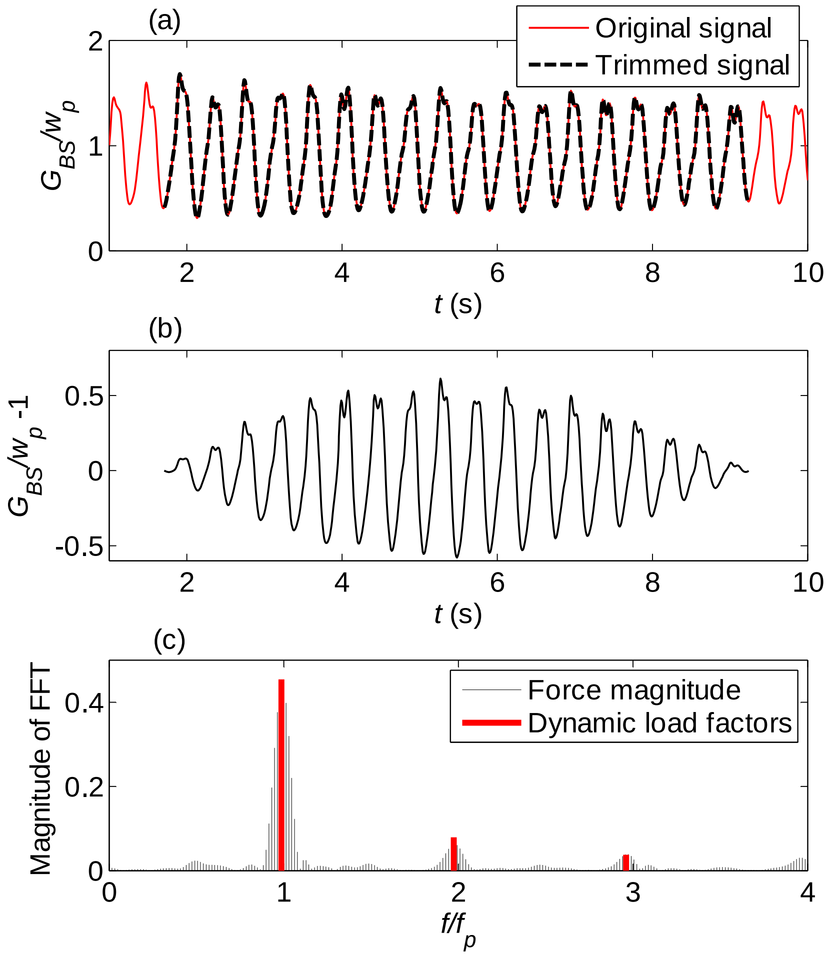

Figure 12 Determination of walking DLFs: (a) Tekcsan original and trimmed force signal (b) windowed trimmed signal (b) Fast Fourier Transform of the trimmed signal with frequency resolution, 0.01 Hz (the variability in FFT might not be representative of normal walking due to setting the pacing frequency with the metronome, and some of the energy spread to adjacent frequencies is due to leakage from the use of the Hann window).

For each trial and surface (rigid and bridge surface), first two DLFs of pedestrian force are calculated. Then, the mean DLF is taken across the five trials for each test subject for a specific pacing frequency. Figure 13 illustrates the mean first and second DLF for different frequency ratios and mass ratios (the grey regions show Kerr's DLFs [46]). As seen in Figure 13a, for the resonance case, β = 1, the difference between the mean first DLF of the rigid and bridge surfaces is significant. As the mass ratio increases, this difference tends to increase. However, the difference is not monotonically increasing. From Figure 13b, it is clear that, for resonances by both first and second harmonic, β = 1 and β = 0.5, there is a substantial difference between second mean DLFs of rigid and bridge surface. Furthermore, the DLFs on the bridge surface are smaller than those on the rigid surface for $\beta = 1$. When β becomes far from 1 (i.e. $\beta = 0.87$, 0.5), the difference in first DLFs gets smaller, and it seems that the vibrating bridge does not have a significant effect on the mean DLFs. The second DLFs of the bridge surface are smaller than those of the rigid surface for both resonance and second harmonic excitation, $\beta = 1$ and $\beta = 0.5$. Considering then the postulated S2HI effect, the bridge surface DLFs can be expressed as:

$$\mathrm{DLF}_{BS} = \mathrm{DLF}_{RS} - \Delta\mathrm{DLF}_{\mathrm{S2HI}} \tag{2}$$

which DLF_{BS} and DLF_{RS} are dynamic load factors of human force on bridge and rigid surfaces, respectively; $\Delta\mathrm{DLF}_{\mathrm{S2HI}}$ is the change in the dynamic force due to the S2HI effects caused by the vibration. It should be mentioned that as the test subject gets heavier, this effect typically becomes more pronounced.

The drop in DLF_1 on the lively surface was also found in [47], [23] in which it was explained as being a consequence of a vibration-induced 'self-excited force'. This concept suggests that there are two components combine to give the GRF on the bridge surface, G_{BS}: rigid surface force, G_{RS} and S2HI force component, G_{S2HI}. However, there is not yet an accepted definition of what amount of HSI is to be characterized as "self-excited".

This paper has been published under the following reference: Ahmadi, E., Caprani, C., Živanović, S., Evans, N. and Heidarpour, A. (2018) A framework for quantification of human-structure interaction in vertical direction. *Journal of Sound and Vibration*, Vol. 432, pp. 351-372. (https://doi.org/10.1016/j.jsv.2018.06.054)

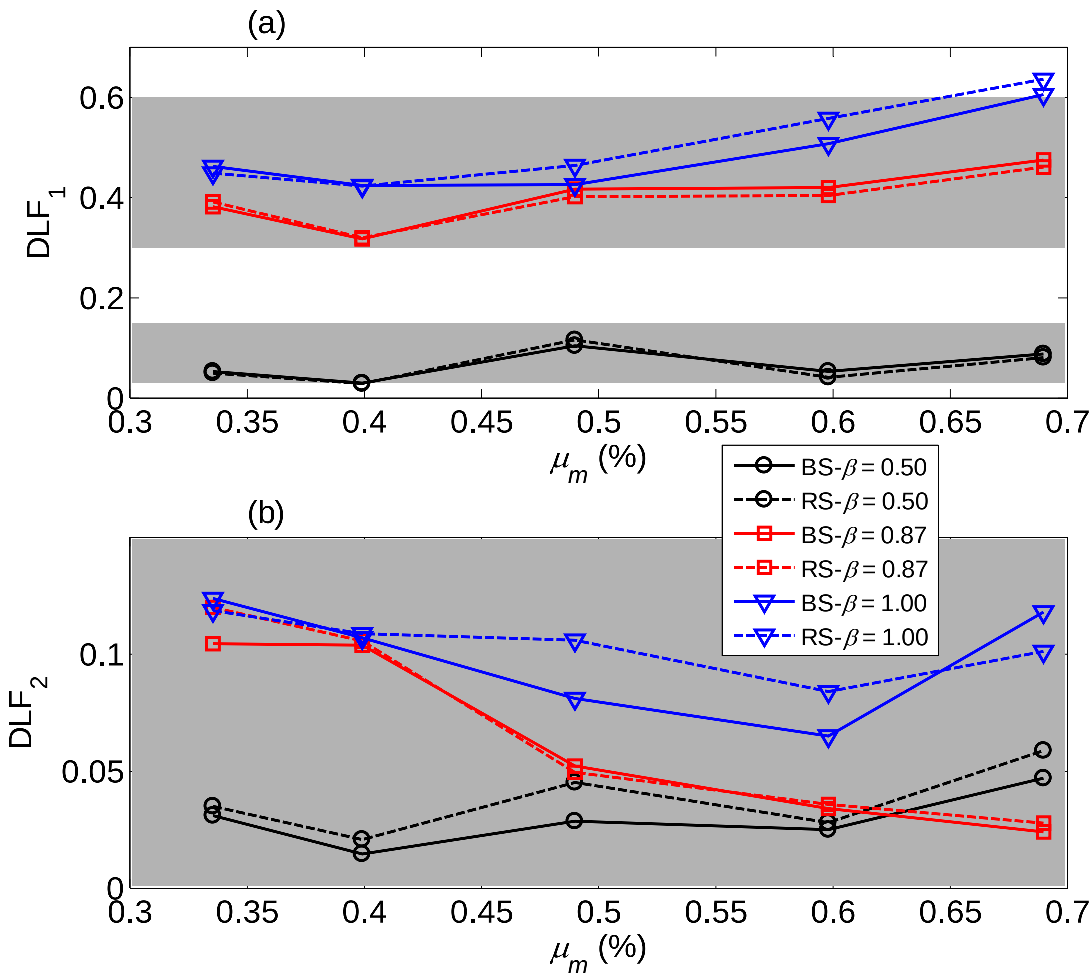

Figure 13 Mean dynamic load factor of (a) first harmonic (b) second harmonic versus mass ratio for different frequency ratios, showing Kerr's [46] DLF regions (greyed) (RS and BS stand for rigid surface and bridge surface respectively).

4.2 Simulated and measured vibration response

The analytical model used to simulate vibration response is shown in Figure 14. The pedestrian is modelled as a force moving at constant velocity and the bridge is modelled as a simply-supported beam in modal space considering only the first mode of the vibration. The measured force, $G(t)$, moving at the actual average velocity as recorded in each trial is used in simulations. As previously mentioned, the bridge frequency and damping are amplitude-dependent, and this is considered in the numerical model.

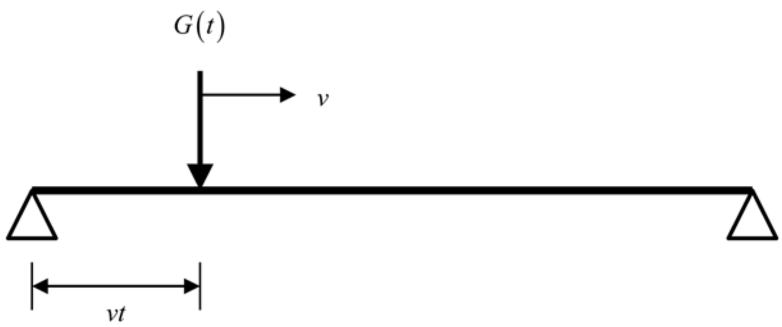

Figure 14 Analytical modelling of human-bridge system.

The equation of motion in modal space is [24]:

$$\ddot{q}(t)+2\xi_b\omega_b\dot{q}(t)+\omega_b^{2}q(t)=\frac{\phi(x)G(t)}{M_b}\delta(x-vt) \tag{3}$$

where q, $\dot{q}$ and $\ddot{q}$ are the modal displacement, velocity, and acceleration for the first mode of the bridge; ξ_b and ω_b are the vibration amplitude-dependent damping and circular frequency of the first mode; they are updated for each amplitude of vibration [48]; M_b and $\phi(x)$ are the modal mass and mode shape; $G(t)$ is the measured human force on either rigid or bridge surface (G_{RS} or G_{BS}); δ is Dirac delta function; x is a position on the bridge; and vt is the pedestrian location at time t, while v is the average velocity of the traverse. The modal vibration response of the bridge is obtained using Newmark-β integration. Finally, vibration response of the bridge in physical coordinates at any location is given by:

$$\ddot{u}(x,t)=\varphi(x)\ddot{q}(t) \tag{4}$$

where the mode shape can be approximated by a half-sine function [49]:

$$\varphi(x)=\sin\left(\frac{\pi x}{L}\right) \tag{5}$$

where L is the bridge length. Figure 15a shows the measured vibration response and simulated RS, and BS responses at the bridge mid-span for the exemplary test subject. The measured

This paper has been published under the following reference: Ahmadi, E., Caprani, C., Živanović, S., Evans, N. and Heidarpour, A. (2018) A framework for quantification of human-structure interaction in vertical direction. *Journal of Sound and Vibration*, Vol. 432, pp. 351-372. (https://doi.org/10.1016/j.jsv.2018.06.054)

accelerations are seen to be smaller than that simulated by the numerical model, even when using the measured induced force to the bridge surface. The difference between the peak amplitudes of measured and both forms of simulated vibrations for the exemplary test subject are shown in Figure 15b. The differences between the RS and BS responses as well as between the measured and BS responses become more and more obvious as the response amplitude increases. However, these differences have sporadic increasing and decreasing trends. Further, in this example, the difference is far more significant between measured and BS responses, than between RS and BS responses.

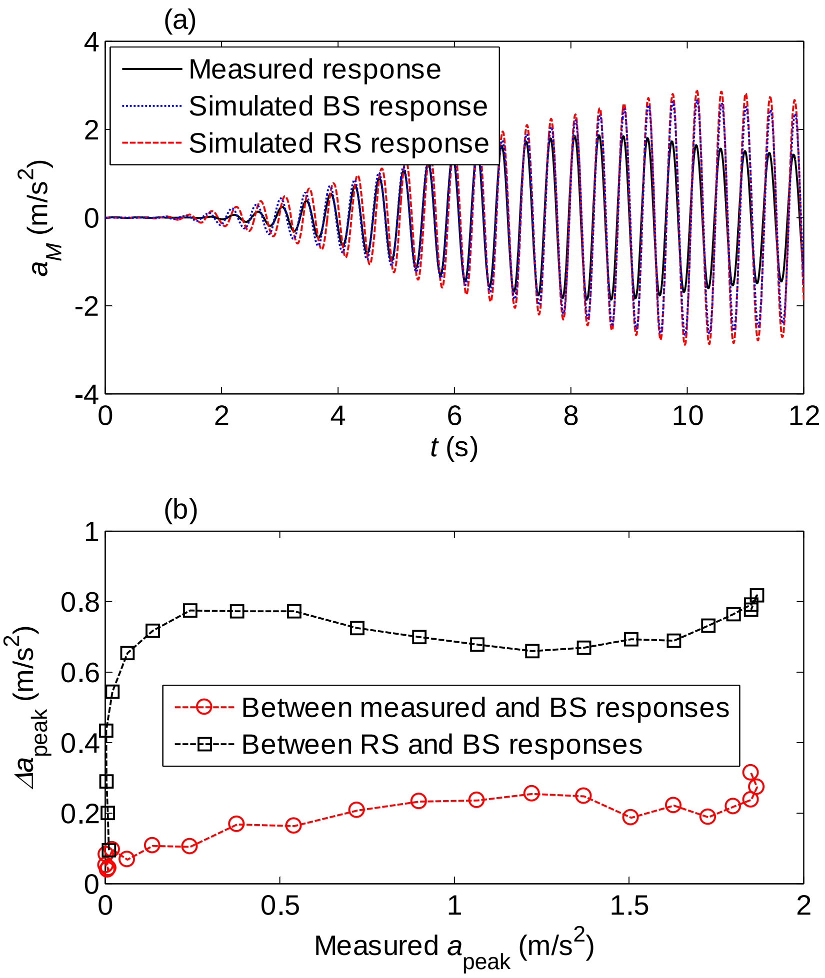

Figure 15 (a) Measured response (from the experiment), simulated BS, and RS responses (from the numerical model) (b) differences beetwen peak amplitudes of the responses of (a) – see Figure 2 for meaning.

The maximum of each acceleration time history, a_{max}, is used as a response metric. Maximum root-mean-square (RMS) could be used instead, but is directly proportional to the peak

This paper has been published under the following reference: Ahmadi, E., Caprani, C., Živanović, S., Evans, N. and Heidarpour, A. (2018) A framework for quantification of human-structure interaction in vertical direction. *Journal of Sound and Vibration*, Vol. 432, pp. 351-372. (https://doi.org/10.1016/j.jsv.2018.06.054)

acceleration over a few cycles of vibration, and so response ratios are unaffected by the measure used. The results are given in Tables 3 (RS responses) and 4 (BS responses), and shown in Figure 16. The variability of results is low with coefficient of variation up to 0.29 and central tendencies are therefore meaningful to describe the results.

Table 3. Maximum acceleration response (a_{max}, m/s^2) of the numerical model using the measured rigid surface GRFs.

Test Subject	Mass Ratio, μ_m (%)	Frequency Ratio, β	Trial No.					Mean
			1	2	3	4	5	
1	0.33	0.50	0.10	0.24	0.18	0.16	0.18	0.17
		0.87	0.17	0.19	0.24	0.15	0.19	0.19
		1.00	1.13	1.34	1.29	1.53	1.45	1.35
2	0.40	0.50	0.14	0.13	0.16	0.16	0.11	0.14
		0.87	0.17	0.18	0.21	0.15	0.15	0.17
		1.00	1.38	1.31	1.49	1.52	1.52	1.44
3	0.50	0.50	0.14	0.14	0.14	0.16	0.15	0.15
		0.87	0.34	0.23	0.31	0.33	0.23	0.29
		1.00	2.06	2.02	1.97	1.79	1.68	1.90
4	0.60	0.50	0.27	0.29	0.25	0.22	0.26	0.26
		0.87	0.33	0.31	0.29	0.31	0.32	0.31
		1.00	2.98	2.28	3.11	2.95	2.96	2.86
5	0.70	0.50	0.63	0.56	0.65	0.53	0.42	0.56
		0.87	0.36	0.38	0.42	0.34	0.42	0.38
		1.00	2.19	3.36	1.62	3.48	2.91	2.71

Table 4. Maximum acceleration response (a_{max}, m/s^2) of the numerical model using the measured bridge surface GRFs.

Test Subject	Mass Ratio, μ_m (%)	Frequency Ratio, β	Trial No.					Mean
			1	2	3	4	5	
1	0.33	0.50	0.22	0.23	0.12	0.24	0.21	0.20
		0.87	0.17	0.25	0.22	0.19	0.18	0.20
		1.00	1.31	1.42	1.31	1.38	1.34	1.35
2	0.40	0.50	0.09	0.06	0.09	0.07	0.06	0.07
		0.87	0.17	0.19	0.16	0.14	0.08	0.15
		1.00	1.10	1.53	1.46	1.37	1.27	1.35
3	0.50	0.50	0.17	0.21	0.12	0.11	0.15	0.15

This paper has been published under the following reference: Ahmadi, E., Caprani, C., Živanović, S., Evans, N. and Heidarpour, A. (2018) A framework for quantification of human-structure interaction in vertical direction. *Journal of Sound and Vibration*, Vol. 432, pp. 351-372. (https://doi.org/10.1016/j.jsv.2018.06.054)

		0.87	0.37	0.26	0.30	0.26	0.24	0.28
		1.00	1.65	1.07	1.76	1.51	1.59	1.52
		0.50	0.23	0.20	0.19	0.30	0.27	0.24
4	0.60	0.87	0.27	0.29	0.25	0.22	0.26	0.26
		1.00	1.54	1.86	2.42	2.27	2.68	2.15
		0.50	0.47	0.49	0.47	0.59	0.65	0.53
5	0.70	0.87	0.29	0.40	0.44	0.32	0.39	0.37
		1.00	3.22	3.29	3.62	3.26	3.26	3.33

To perform further analysis and understand the central tendency of the simulated and measured responses, an average is taken across trials for each test subject with a specific pacing frequency, and it is shown in the last column of Tables 3 and 4. For $\beta = 1$ the RS response is greater than the BS response for almost all test subjects except for the test subject with mass ratio 0.70%. The BS response is significantly larger than the measured response for all cases at frequency ratio of 1. As shown in the experimental-numerical programme (Figure 2), these differences between RS and BS responses, and between BS and measured responses reflect S2HI and H2SI, respectively. Hence, excluding S2HI and H2SI overestimates vibration response by up to 32% and 33%, respectively (see Figure 16c).

The overestimation of vibration response as a result of ignoring both HSI forms may lead to vibration serviceability assessment failure of a bridge, while it may in truth be serviceable. Both S2HI and H2SI effects increase as frequency ratio and mass ratio increase (Figure 16c). For S2HI, it means that its influence on the walking force acting on the bridge surface increases, both as the vibration amplitude tends to increase and as the test subject gets heavier. For H2SI, the effects of the test subjects' mass and pacing frequency support the hypothesis that the human body can act as a dynamic absorber. When the pacing frequency of the test subject (absorber frequency) is close to the bridge frequency, the energy dissipated by the pedestrian

This paper has been published under the following reference: Ahmadi, E., Caprani, C., Živanović, S., Evans, N. and Heidarpour, A. (2018) A framework for quantification of human-structure interaction in vertical direction. *Journal of Sound and Vibration*, Vol. 432, pp. 351-372. (https://doi.org/10.1016/j.jsv.2018.06.054)

increases. Also, as the test subject (absorber) gets heavier, it seems that more energy is damped out of the bridge.

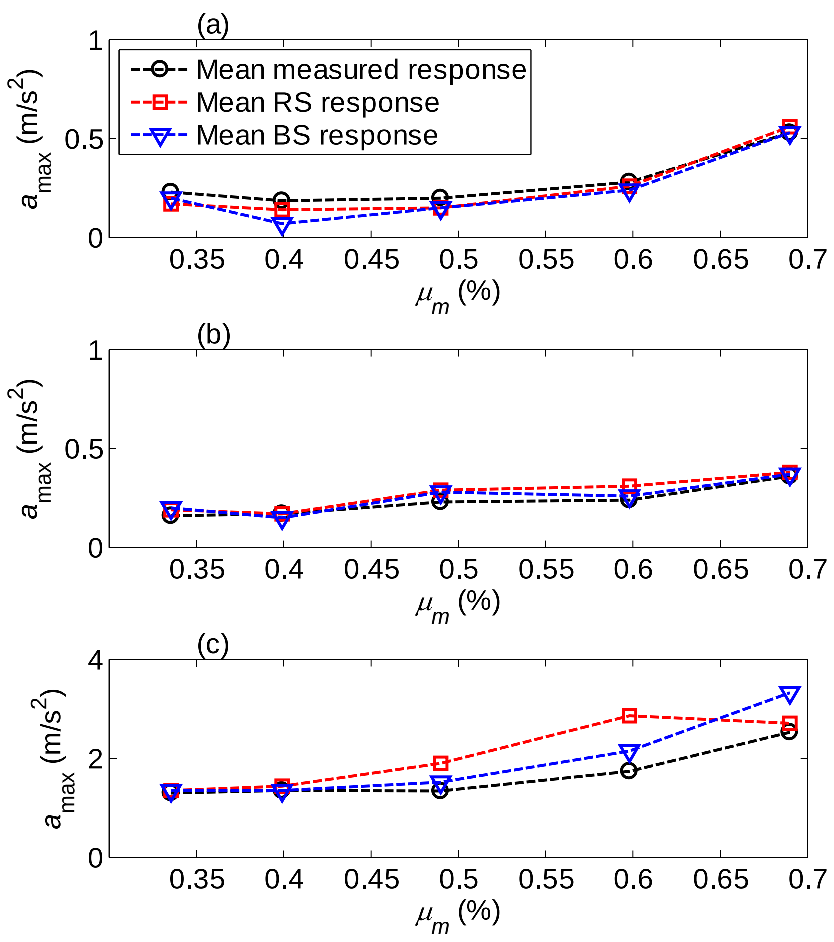

Figure 16 Mean maximum acceleration for frequency ratio of: (a) 0.50 (b) 0.87 (c) 1. See Figure 2 to understand why the blue (BS) to black (measured) lines reflects the effect of H2SI and red (RS) to blue, that of S2HI.

5. Statistical Tests

In section 4.2, it was shown that the differences between mean responses are large at resonance. These differences are an indication of HSI as per Figure 2. However, two important caveats must be considered regarding the results. First, a small number of five trials for each test subject and pacing frequency was used to calculate the mean maximum acceleration response for the simulated RS and BS vibration response and measured vibration response. The question then is, to what extent the small number of trials reflect the real (population) difference between

This paper has been published under the following reference: Ahmadi, E., Caprani, C., Živanović, S., Evans, N. and Heidarpour, A. (2018) A framework for quantification of human-structure interaction in vertical direction. *Journal of Sound and Vibration*, Vol. 432, pp. 351-372. (https://doi.org/10.1016/j.jsv.2018.06.054)

mean vibration responses. In other words, are the differences in means by chance or representative of the population of responses as a whole? To answer this, parametric statistical hypothesis testing is used. Second, careful consideration must be given to measurement inaccuracies input to the numerical model which consequently influence the simulated vibration responses. To quantify this, the input parameters are described in terms of probability density functions (PDFs) and Monte Carlo simulations of output responses conducted. This allows a broader understanding of the differences between the results, and hence the quantitative influence of HSI in a probabilistic sense.

5.1 Parametric test (hypothesis test)

A parametric test makes assumptions about the underlying distribution of the population from which the sample is being drawn. The population distribution of responses is assumed to be normal, which can be reasonably justified through the central limit theorem [50]. According to the experimental-numerical programme (Figure 2), the null, H_0, and alternative hypotheses, H_1, for each HSI form are given as:

1) S2HI:

$$\begin{cases} H_0: & \overline{R}_{RS} - \overline{R}_{BS} = 0 \\ H_1: & \overline{R}_{RS} - \overline{R}_{BS} \neq 0 \end{cases} \tag{6}$$

2) H2SI:

$$\begin{cases} H_0: & \overline{R}_{BS} - \overline{R}_{M} = 0 \\ H_1: & \overline{R}_{BS} - \overline{R}_{M} \neq 0 \end{cases} \tag{7}$$

where $\overline{R}_{RS}$, $\overline{R}_{BS}$, and $\overline{R}_{M}$ stand for the mean response metric for the simulated RS, BS, and measured cases respectively for a large population of trials. If null hypothesis, H_0, is correct it means that HSI is not significant, and that the difference in the means of two small samples are

This paper has been published under the following reference: Ahmadi, E., Caprani, C., Živanović, S., Evans, N. and Heidarpour, A. (2018) A framework for quantification of human-structure interaction in vertical direction. *Journal of Sound and Vibration*, Vol. 432, pp. 351-372. (https://doi.org/10.1016/j.jsv.2018.06.054)

by chance; otherwise, the alternative hypothesis, H_1, is more likely and HSI exists in the population of vibration responses.

When performing the hypothesis test, no HSI (null hypothesis) might be reached or two errors could be made: incorrectly accepting HSI when it does not exist (error of the first kind) or rejecting it when it does exist (error of the second kind). It is desirable to minimize the probabilities of the two types of error. However, these errors cannot be controlled. Therefore, a level of significance, α, is assigned to the probability of incorrectly accepting HSI when it does not exist and then the error due to rejecting HSI when it does exist is minimized. The standard way to remove the arbitrary choice of α is to report the p-value of the test, defined as the smallest level of significance leading to accepting the alternative hypothesis (i.e. that HSI exists). The p-value gives an idea of how strongly the data contradicts the hypothesis that there is no HSI of any form. A small p-value shows that the mean response metrics are highly likely to be different, and hence HSI exists.

To test the difference between the two samples for each form of HSI (see Figure 2 and equations (6) and (7)), the two-sided independent sample Student's t-test is used, with equal variances assumed for both populations. Table 5 summarizes the hypothesis test results for both HSI forms for each pacing frequency, as assessed using the maximum acceleration response metric (Tables 1, 3, and 4). It is clear that HSI only has significance for the $\beta = 1$ case (for which p-values are small) while for the other frequency ratios, HSI mostly does not have a statistically significant effect on the result. Considering then just the resonant case, for both HSI forms, it can be seen that higher mass ratios mostly gives smaller p-values. This means that the effect of HSI effect increases with mass ratio (as may be expected). However, typically p-values resulting from H2SI, especially for heavy test subjects, are smaller than those of S2HI, indicating that the effect of HSI on the dynamic properties of the system is more pronounced than the effect of the structure on the pedestrian walking force. There are some unexpected cases though for the mass ratios of 0.40% and 0.50%. Nevertheless, overall for the resonant case ($\beta = 1$), the results give strong support to the existence of H2SI, and somewhat weaker support to S2HI and show that the mass ratio is an important factor.

Table 5. *p*-values for the two postulated forms of HSI from the *t*-test for the maximum acceleration metric.

Test Subject	μ_m (%)	$\beta = 0.5$		$\beta = 0.87$		$\beta = 1$	
		S2HI	H2SI	S2HI	H2SI	S2HI	H2SI
1	0.33	0.33	0.40	0.52	0.35	0.96	0.29
2	0.40	0.41	0.54	0.30	0.10	0.29	0.67
3	0.50	0.75	0.19	0.95	0.25	0.02	0.17
4	0.60	0.43	0.24	0.72	0.92	0.05	0.02
5	0.70	0.67	1.00	0.63	0.97	0.13	0.00

5.2 Non-parametric test (Monte Carlo Simulation)

Non-parametric testing is used to determine the effects of measurement and model errors on the numerical model vibration response, and hence the conclusions drawn from these results. Such errors could affect the HSI quantification, since the postulated HSI forms are defined in terms of differences between simulated and measured responses. Figure 17 illustrates a schematic view of potential errors in the experimental-numerical programme (also refer to Figure 2). It includes the real bridge, numerical model inputs and outputs, as well as errors. The first type of error is measurement error. G_{BS}^{R} is the real (true) force without any error inputted into the real bridge. R_M is the measured response of the bridge with possible error, ε_a, for one walking trial. This error is assumed negligible as the accelerometers used to measure the bridge response (Honeywell QA750) are of very high quality, with very low noise floor and output frequency response down to DC. The final measurement error is due to the GRF

This paper has been published under the following reference: Ahmadi, E., Caprani, C., Živanović, S., Evans, N. and Heidarpour, A. (2018) A framework for quantification of human-structure interaction in vertical direction. *Journal of Sound and Vibration*, Vol. 432, pp. 351-372. (https://doi.org/10.1016/j.jsv.2018.06.054)

measurement system, TekScan, denoted ε_G, which influences the measured pedestrian forces, G_{BS} and G_{RS}.

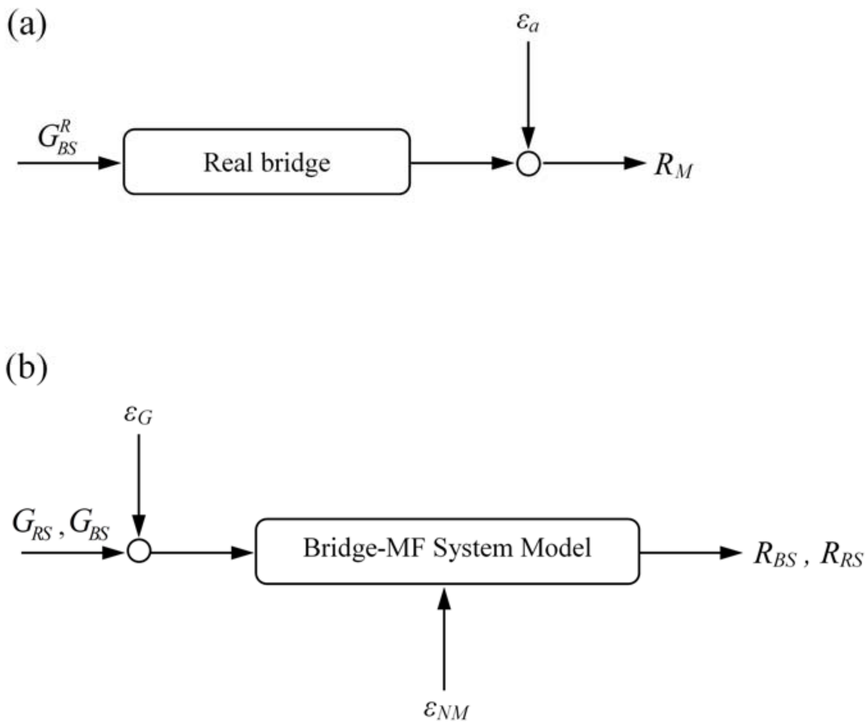

Figure 17 Schematic view of errors for: (a) real bridge (b) numerical model.

The second type of error is the error of the numerical model, ε_{NM}, which reflects the ability of the (simple) model to replicate reality. This error emanates from many possible sources which do occur but are not adequately captured in the model, such as the actual damping, frequency, mass, frictions/nonlinearities, nonlinear material behaviour, etc. In particular, the effects of the bridge damping and frequency are significant at resonance: small changes in these strongly affect the vibration response and so these are considered in detail. Each considered model parameter error is defined as:

$$\varepsilon\left(X\right)=\frac{X_{BM}-X}{X} \tag{8}$$

where X_{BM} is the benchmark value for the parameter, X. For the bridge damping and frequency, the free vibration results at the end of each trial were taken as the benchmark values, which is

This paper has been published under the following reference: Ahmadi, E., Caprani, C., Živanović, S., Evans, N. and Heidarpour, A. (2018) A framework for quantification of human-structure interaction in vertical direction. *Journal of Sound and Vibration*, Vol. 432, pp. 351-372. (https://doi.org/10.1016/j.jsv.2018.06.054)

reasonable since any ε_a is extremely small as noted above. Thus, the errors are estimated for the bridge damping and frequency using equation (8). Kernel density estimation is then used to estimate the PDF of the errors for each variable [51]. Figure 18 shows the PDFs of the errors for bridge frequency and damping.

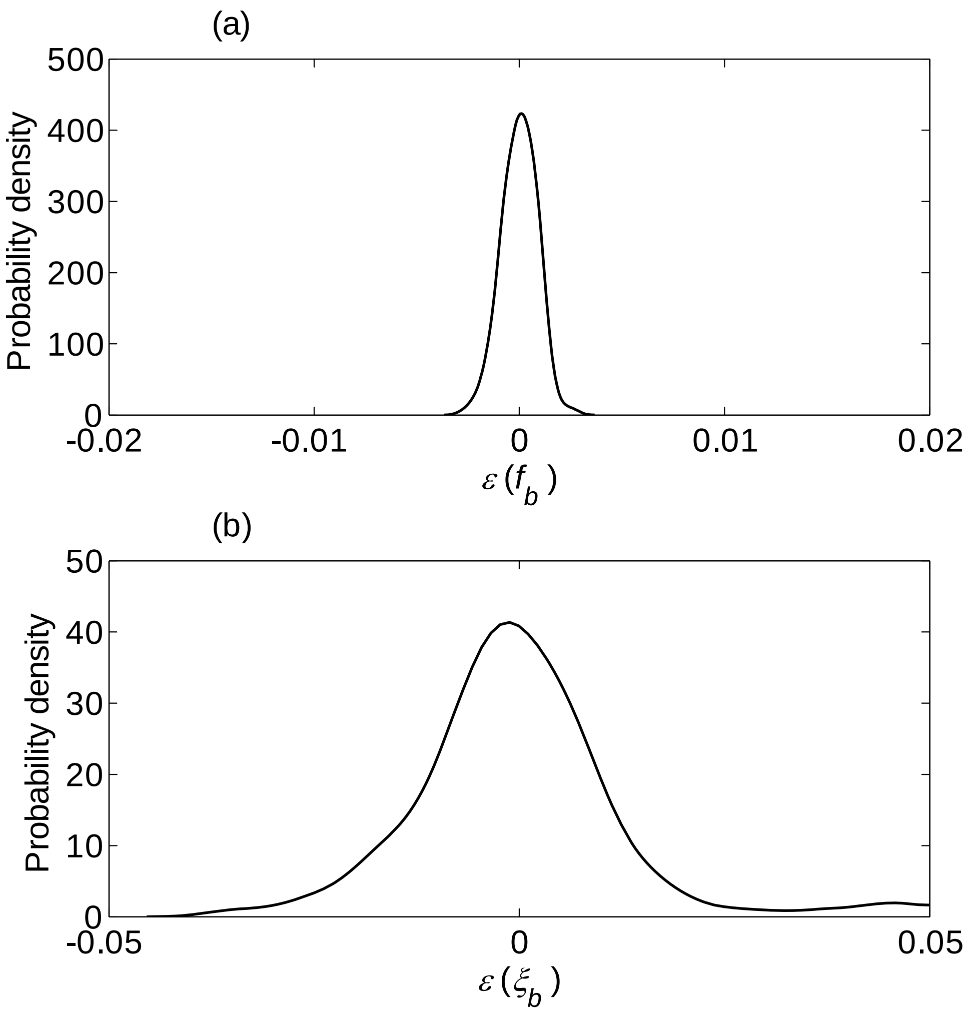

Figure 18 Probability density of bridge: (a) frequency (b) damping.

For the GRFs, the results of the force plate are treated as the benchmark or 'true' values. The Tekscan system generally gives different force estimate. To model the true force from the Tekscan measurements, the Tekscan error is analysed statistically. Since the sample rate is the same for both the force plate and Tekscan, time is indicated by the index, i. Index j is used to denote a specific trial of which there are N. The Tekscan measurement relative error for trial j at time i is:

$$\varepsilon_{ij} = \frac{G_{ij}^{FP} - G_{ij}^{TS}}{G_{ij}^{TS}} \tag{9}$$

Figure 19a shows the histogram of εij for all trials, and Figure 19b illustrates the probability density of the relative errors using Kernel density estimation [51]. As a conservative estimation of the Tekscan error, this probability density function is used to generate relative random errors, ε_i, which are employed to generate random representative force plate footsteps:

$$G_i^{FP} = \left(1+\varepsilon_i\right) G_i^{TS} \tag{10}$$

Finally, randomly generated representative force plate footsteps are combined to create a continuous force plate GRF.

Using this procedure for input force, and PDFs (Figure 18) for bridge frequency, and damping, 10^4 Monte Carlo simulations (MCSs) are performed to determine the variability of results due to these possible errors. It is emphasized that the PDFs used are nonparametric (i.e. directly those of Figures 18 and 19b), and so no additional error is introduced by assuming a parametric PDF form (e.g. normal, lognormal).

This paper has been published under the following reference: Ahmadi, E., Caprani, C., Živanović, S., Evans, N. and Heidarpour, A. (2018) A framework for quantification of human-structure interaction in vertical direction. *Journal of Sound and Vibration*, Vol. 432, pp. 351-372. (https://doi.org/10.1016/j.jsv.2018.06.054)

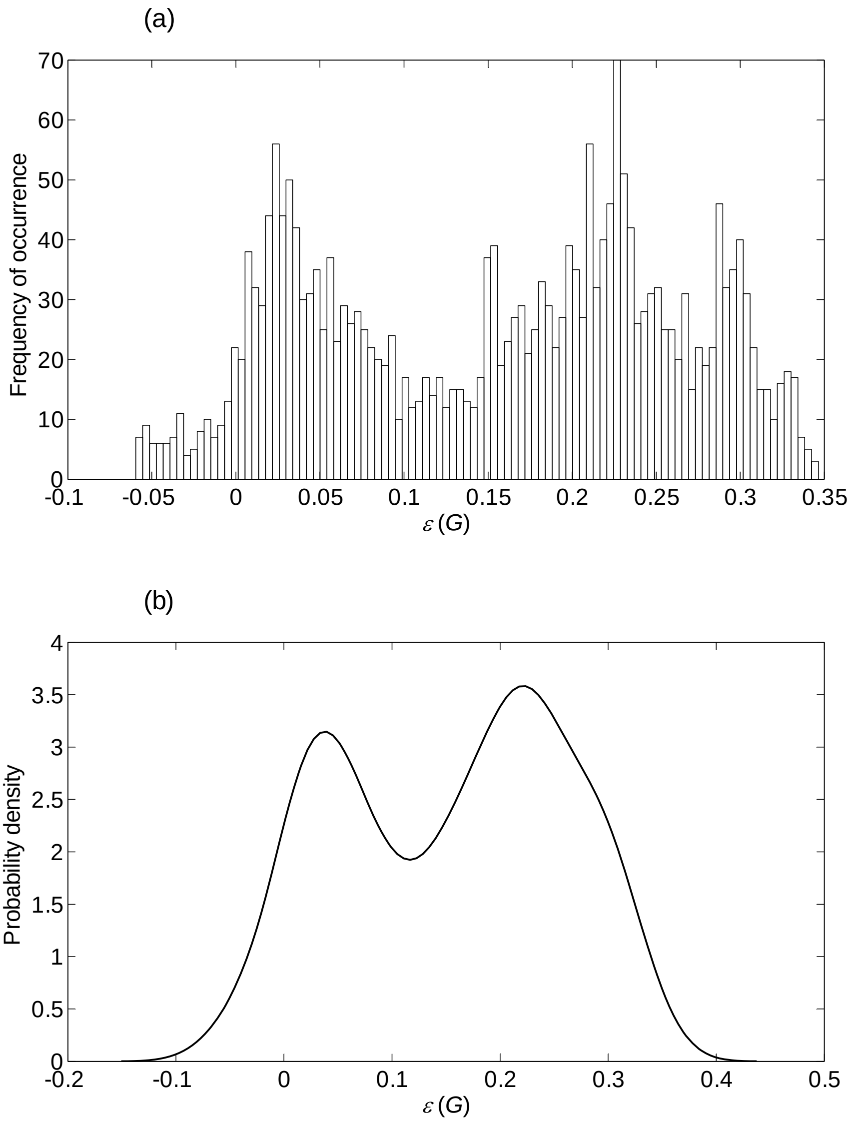

Figure 19. Tekscan measurement relative error: (a) histogram (b) probability density.

By way of example, Figure 20 shows the resulting histograms for possible RS and BS responses considering the model errors, along with the actual corresponding measured response for the exemplary test subject. The figure suggests that the RS and BS response distributions are strongly biased with respect to the measurement. This is due to the very wide error distribution taken for the Tekscan error; unfortunately no better error model is available. Nevertheless, in a relative sense, there is a difference between the distributions for RS and BS forces. According to the experimental-numerical framework of Figure 2, this then, is the influence of HSI.

This paper has been published under the following reference: Ahmadi, E., Caprani, C., Živanović, S., Evans, N. and Heidarpour, A. (2018) A framework for quantification of human-structure interaction in vertical direction. *Journal of Sound and Vibration*, Vol. 432, pp. 351-372. (https://doi.org/10.1016/j.jsv.2018.06.054)

Further, the distance between the mean and measurement reflects to some extent the error of the state-of-the-art practice (Figure 2).

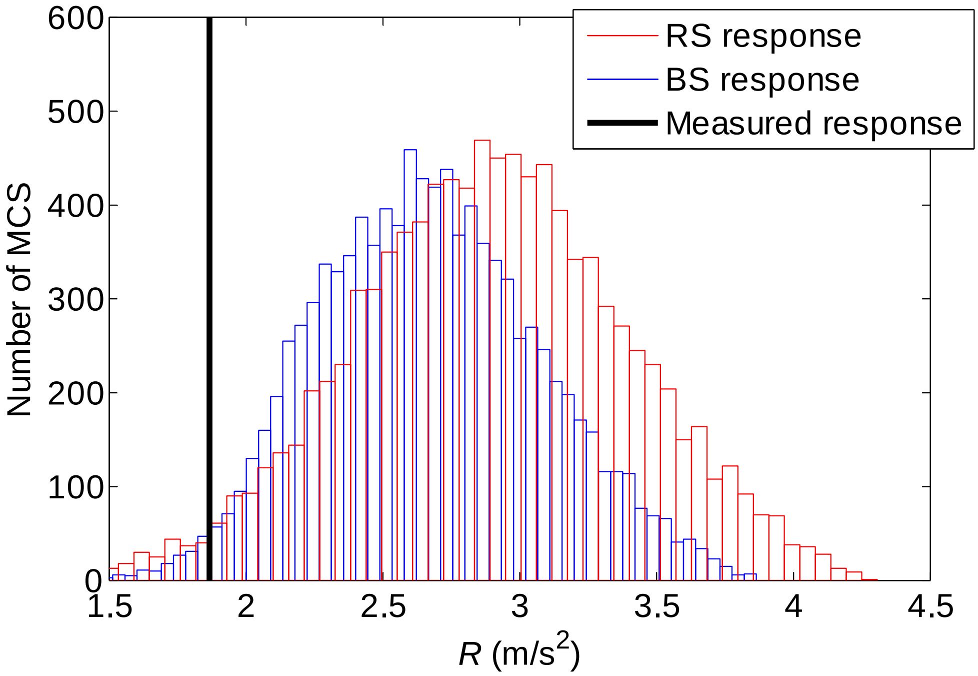

Figure 20 Histograms for RS and BS responses from MCS which considers possible measurement errors, and the corresponding measured vibration response.

To quantify the HSI effect, the relative difference between the vibration responses is defined based again on Figure 2. Thus, for S2HI we have:

$$\Delta_{\mathrm{S2HI}} = \frac{\mathbf{R}_{RS} - \mathbf{R}_{BS}}{R_M} \tag{11}$$

and for H2SI:

$$\Delta_{\mathrm{H2SI}} = \frac{\mathbf{R}_{BS} - R_M}{R_M} \tag{12}$$

in which $\mathbf{R}_{RS}$ and $\mathbf{R}_{BS}$ are the vectors of simulated random responses for the RS and BS surfaces, respectively obtained from MCS. Then, PDFs are constructed for each trial individually, as well as for the group of 5 trials as a whole (merged trials). Figure 21 shows the PDFs for the exemplary test subject for each individual trial and the merged trials. It is clear

This paper has been published under the following reference: Ahmadi, E., Caprani, C., Živanović, S., Evans, N. and Heidarpour, A. (2018) A framework for quantification of human-structure interaction in vertical direction. *Journal of Sound and Vibration*, Vol. 432, pp. 351-372. (https://doi.org/10.1016/j.jsv.2018.06.054)

that most of the randomly realized Δ-values for both HSI forms are non-zero and positive, indicating the relative influence of HSI. The grey filled areas represent the probability of HSI non-existence or negative effect (negative side of the probability curves). In this example, this probability is 20% and 5% for S2HI and H2SI respectively, again reflecting that both are likely to exist and that H2SI is by far the stronger effect.

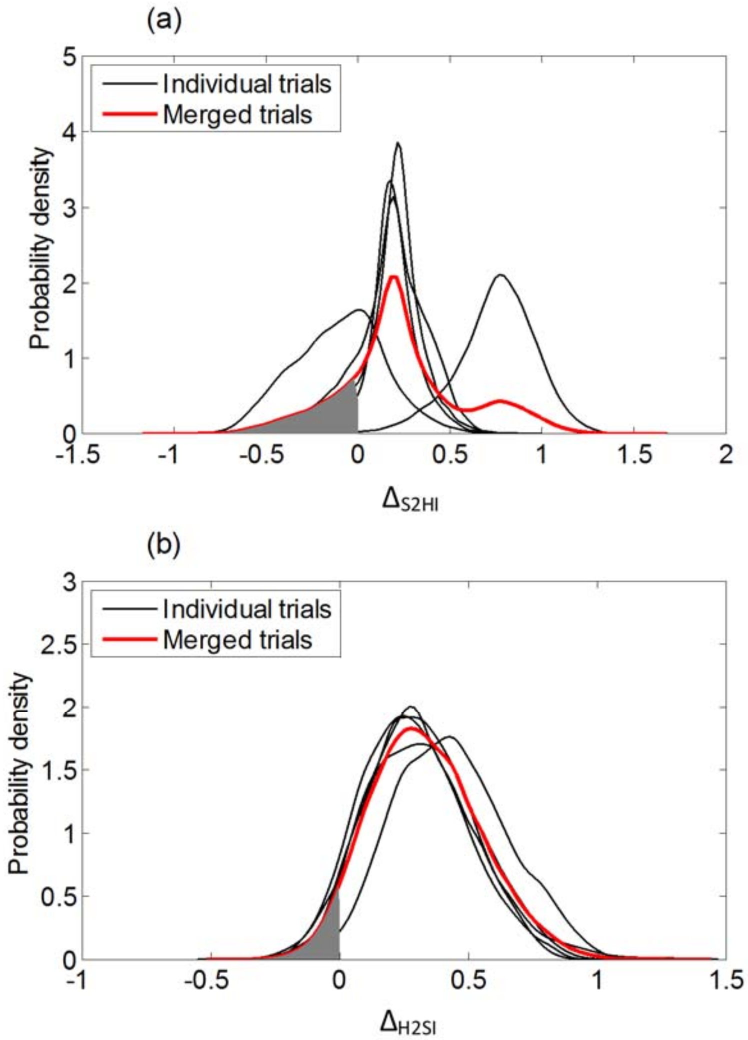

Figure 21 Probability density for the exemplary test subject at resonance for (a) S2HI (b) H2SI.

The effects of both HSI forms on vibration response can be given as:

$$R_M = \frac{R_{RS}}{1+\Delta_{\mathrm{HSI}}} \tag{13}$$

This paper has been published under the following reference: Ahmadi, E., Caprani, C., Živanović, S., Evans, N. and Heidarpour, A. (2018) A framework for quantification of human-structure interaction in vertical direction. *Journal of Sound and Vibration*, Vol. 432, pp. 351-372. (https://doi.org/10.1016/j.jsv.2018.06.054)

where,

$$\Delta_{\mathrm{HSI}} = \Delta_{\mathrm{S2HI}} + \Delta_{\mathrm{H2SI}} \tag{14}$$

The vibration response based on RS measurements is reduced by a factor to reach the measured vibration response. The most likely values of Δ_{S2HI} and Δ_{H2SI} are identified as the modes of the PDFs similar to Figure 21. These values are 0.21 and 0.27 for the exemplary test subject (Figure 21) giving a combined factor of 0.67 (as just one example). That is, the measured response is 67% of that estimated using rigid surface GRFs and a moving force numerical model (even allowing for amplitude-dependent damping). Table 6 shows these results for each test subject for the case at resonance only, since this is when HSI has most effect. The results show that HSI has a significant effect, and it increases with mass ratio. With further experiments, results of this nature could be used to provide more accurate vibration serviceability models that account for HSI.

Table 6. Relative and combined influence of HSI types (refer to equations (13) and (14)).

Test Subject	$\mu\mu\mu_m$ (%)	Δ_{S2HI}	Δ_{H2SI}	Δ_{HSI}	R_M/R_{RS}
1	0.33	0.03	0.02	0.05	0.95
2	0.40	0.03	0.04	0.07	0.93
3	0.50	0.12	0.17	0.29	0.77
4	0.60	0.21	0.27	0.48	0.67
5	0.70	0.10	0.28	0.38	0.72

6. Conclusions

In this paper, the human-structure interaction phenomenon was quantified using a novel experimental-numerical approach. The imparted footfall force to both rigid and bridge surface was measured along with the resulting bridge response. The moving force model was adopted to simulate vibration as a commonly-used model in design codes which ignores human-structure interaction. The difference between simulated and measured responses as well as the

This paper has been published under the following reference: Ahmadi, E., Caprani, C., Živanović, S., Evans, N. and Heidarpour, A. (2018) A framework for quantification of human-structure interaction in vertical direction. *Journal of Sound and Vibration*, Vol. 432, pp. 351-372. (https://doi.org/10.1016/j.jsv.2018.06.054)

difference between dynamic load factors of the forces on the rigid and bridge surface were used as criteria to evaluate HSI existence.

It was found that human-structure dynamic interaction is associated both with the forces that excite the structure (S2HI) and with the corresponding influence of humans on the dynamic properties of the structure they occupy (H2SI). H2SI is found to be a far stronger influence than S2HI for the bridge studied. The intensity of both S2HI and H2SI is found to increase as the mass ratio between the human and structure increases. At resonance, where vibration amplitude reaches its peak, the HSI effects are the most pronounced. The results of parametric statistical hypothesis testing show that HSI is of statistical significance, and H2SI is very likely in particular. Furthermore, non-parametric testing was done to see the effects of numerical model and measurement errors on HSI existence. It shows that HSI remains of statistical significance even accounting for numerical model and measurement errors. Similar to the parametric test, it is found that H2SI is more statistically significant than S2HI. This approach enabled a probabilistic quantification of both HSI effects, as well as their combined effect. Such an approach could prove useful in adapting the moving force model to give results that compare better to measurements.

The Warwick Bridge has a low pedestrian-to-bridge mass ratio, up to 0.7% in this study. For bridges with higher mass ratios, the intensity of H2SI might be even more significant and pedestrian effects on dynamic properties of the system could be even more pronounced than bridge vibration effects on pedestrian walking force.

This study is a beneficial step forward towards quantifying HSI. It introduces a novel framework which is a combination of an experimental and numerical approach to investigate

This paper has been published under the following reference: Ahmadi, E., Caprani, C., Živanović, S., Evans, N. and Heidarpour, A. (2018) A framework for quantification of human-structure interaction in vertical direction. *Journal of Sound and Vibration*, Vol. 432, pp. 351-372. (https://doi.org/10.1016/j.jsv.2018.06.054)

HSI. The findings provide a means of accounting for human-structure interaction. Such a quantification of HSI could be incorporated into codes of practice rules to improve the accuracy of vibration serviceability assessments.

Acknowledgements

This work was funded by a Monash-Warwick Alliance Seed Grant and a Monash Graduate Scholarship (MGS).

References

[1] Živanović S, Pavic A, Reynolds P. Vibration serviceability of footbridges under human-induced excitation: A literature review. Journal of Sound and Vibration 2005;279:1–74. doi:10.1016/j.jsv.2004.01.019.

[2] Shahabpoor E, Pavic A, Racic V. Interaction between walking humans and structures in vertical direction: a literature review. Shock and Vibration 2016;2016:12–7. doi:10.1155/2016/3430285.

[3] Zammit G V., Menz HB, Munteanu SE. Reliability of the TekScan MatScan®system for the measurement of plantar forces and pressures during barefoot level walking in healthy adults. Journal of Foot and Ankle Research 2010;3:1–9. doi:10.1186/1757-1146-3-11.

[4] Barnett S, Cunningham JL, West S. A Comparison of verical forca and temporal parameters produced by an in-shoe pressure measuring system and a force platform - Barnett.pdf 2001;16:353–7.

[5] Griffin MJ, Erdreich J. Handbook of human vibration. The Journal of the Acoustical Society of America 1991;90:2213. doi:10.1121/1.401606.

[6] Cordero AF. Human gait, stumble and...fall? mechanical limitations of the recovery from a stumble, University of Twente, Enschede, The Netherlands. 2003.

[7] McRobie A, Morgenthal G, Lasenby J, Ringer M. Section model tests on human-structure lock-in. ICE, Bridge Engineering 2003;156:71–9.

[8] Blanchard J, Davies BL, Smith JW. Design criteria and analysis for dynamic loading of footbridges. Proceeding of a Symposium on Dynamic Behaviour of Bridges at the Transport and Road Research Laboratory, Crowthorne, Berkshire, England, 1977.

[9] P. Young. Improved floor vibration prediction methodologies, ARUP vibration seminar. 2001.

[10] Brownjohn JM., Pavic A, Omenzetter P. A spectral density approach for modelling continuous vertical forces on pedestrian structures due to walking. Canadian Journal of Civil Engineering 2004;31:65–77. doi:10.1139/l03-072.

[11] Živanović S, Pavić A, Reynolds P. Probability-based prediction of multi-mode vibration response to walking excitation. Engineering Structures 2007;29:942–54. doi:10.1016/j.engstruct.2006.07.004.

[12] Piccardo G, Tubino F. Simplified procedures for vibration serviceability analysis of footbridges subjected to realistic walking loads. Computers and Structures

2009;87:890–903. doi:10.1016/j.compstruc.2009.04.006.

[13] Venuti F, Racic V, Corbetta A. Modelling framework for dynamic interaction between multiple pedestrians and vertical vibrations of footbridges. Journal of Sound and Vibration 2016;379:245–63. doi:10.1016/j.jsv.2016.05.047.

[14] Racic V, Brownjohn JMW. Stochastic model of near-periodic vertical loads due to humans walking. Advanced Engineering Informatics 2011;25:259–75. doi:10.1016/j.aei.2010.07.004.

[15] Cross R. Standing, walking, running, and jumping on a force plate. American Journal of Physics 1999;67:304. doi:10.1119/1.19253.

[16] Kram R, Griffin TM, Maxwell Donelan J, Hui Chang Y. Force treadmill for measuring vertical and horizontal ground reaction forces. Journal of Applied Physiology 1998;7:764–9. doi:10.1016/j.jacr.2010.07.010.

[17] Weishaupt MA, Hogg HP, Wiestner T, Denoth J, Stüssi E, Auer JA. Instrumented treadmill for measuring vertical ground reaction forces in horses. American Journal of Veterinary Research 2002;63:520–7. doi:10.2460/ajvr.2002.63.520.

[18] Kluitenberg B, Bredeweg SW, Zijlstra S, Zijlstra W, Buist I. Comparison of vertical ground reaction forces during overground and treadmill running. A validation study. BMC Musculoskeletal Disorders 2012;13:235. doi:10.1186/1471-2474-13-235.

[19] Ohlsson SV. Floor vibrations and human discomfort, PhD Thesis, Go¨ teborg, Sweden. Chalmers University of Technology, 1982.

[20] Pavic A, Yu CH, Brownjohn JMW, Reynolds P. Verification of the existence of human-induced horizontal forces due to vertical jumping. Proceedings of IMAC XX, Vol. 1, Los Angeles, CA, February 4–7, 2002, p. 120–6.

[21] Van Nimmen K, Lombaert G, Jonkers I, De Roeck G, Van Den Broeck P. Characterisation of walking loads by 3D inertial motion tracking. Journal of Sound and Vibration 2014;333:5212–26. doi:10.1016/j.jsv.2014.05.022.

[22] Bocian M, Brownjohn JMW, Racic V, Hester D, Quattrone A, Monnickendam R. A framework for experimental determination of localised vertical pedestrian forces on full-scale structures using wireless attitude and heading reference systems. Journal of Sound and Vibration 2016;376:217–43. doi:10.1016/j.jsv.2016.05.010.

[23] Dang HV, Živanovic S. Influence of low-frequency vertical vibration on walking locomotion. Journal of Structural Engineering 2016;142:1–12. doi:10.1061/(ASCE)ST.1943-541X.0001599.

[24] Caprani CC, Ahmadi E. Formulation of human-structure system models for vertical vibration. Journal of Sound and Vibration 2016. doi:http://dx.doi.org/10.1016/j.jsv.2016.05.015.

[25] Busca G, Cappellini A, Manzoni S, Tarabini M, Vanali M. Quantification of changes in modal parameters due to the presence of passive people on a slender structure. Journal of Sound and Vibration 2014;333:5641–52. doi:10.1016/j.jsv.2014.06.003.

[26] Ahmadi E, Caprani CC, Heidarpour A. An equivalent moving force model for consideration of human-structure interaction. Applied Mathematical Modelling 2017;51:526–45. doi:10.1016/j.apm.2017.06.042.

[27] Willford M. Dynamic actions and reactions of pedestrians. Proceedings of the International Conference on the Design and Dynamic Behaviour of Footbridges, Paris, France: 2002, p. 66–73.

[28] Živanović S, Diaz IM, Pavić A. Influence of walking and standing crowds on structural dynamic properties. the 27th IMAC Conference, Orlando, USA: 2009.

[29] Nimmen K Van, Maes K, Živanović S, Lombaert G, Roeck G De, Broeck P Van den. Identification and modelling of vertical human-structure interaction. Proceedings of the 33th International Modal Analysis Conference Series, Orlando: 2015.

[30] Živanović S, Pavić A, Ingólfsson ET. Modeling spatially unrestricted pedestrian traffic on footbridges. Journal of Structural Engineering 2010;136:1296–308. doi:10.1061/(ASCE)ST.1943-541X.0000226.
[31] Caprani CC, Keogh J, Archbold P, Fanning P. Enhancement factors for the vertical response of footbridges subjected to stochastic crowd loading. Computers and Structures 2012;102–103:87–96. doi:10.1016/j.compstruc.2012.03.006.
[32] Kasperski M. Damping induced by pedestrians. the 9th International Conference on Structural Dynamics, EURODYN, Porto, Portugal: 2014, p. 1059–64.
[33] OHBDC, Ontario Highway Bridge Design Code, Highway Engineering Division, Ministry of Transportation and Communication, Ontario, Canada. 1983.
[34] BSI (British Standards Institution). U.K. national annex to Euro- code 1: Actions on structures—Part 2: Traffic loads on bridges. EN 1991-2:2003, London. 2008.
[35] ISO 10137 - Bases for design of structures - Serviceability of buildings and walkways against vibrations. 1992.
[36] Eurocode 5, Design of Timber Structures–Part 2: Bridges, ENV 1995-2: 1997, European Committee for Standardization 1997.
[37] Sétra, Guide methodologique passerelles pietonnes (Technical guide Footbridges: assessment of vibrational behaviour of footbridges under pedestrian loading). 2006.
[38] Design of footbridges – HIVOSS (Human Induced Vibrations of Steel Structures). 2009.
[39] Lasheen MRM, Zivanovic S, Salem E, Dang H V. Static and dynamic performance of a steel-concrete composite bridge. The 9th International Conference on Structural Dynamics, EURODYN, 2014, p. 1007–12.
[40] Forner Cordero A, Koopman HJFM, Van Der Helm FCT. Use of pressure insoles to calculate the complete ground reaction forces. Journal of Biomechanics 2004;37:1427–32. doi:10.1016/j.jbiomech.2003.12.016.
[41] Fong DTP, Chan YY, Hong Y, Yung PSH, Fung KY, Chan KM. Estimating the complete ground reaction forces with pressure insoles in walking. Journal of Biomechanics 2008;41:2597–601. doi:10.1016/j.jbiomech.2008.05.007.
[42] Tekscan, Force Measurement and Tactile Sensors, 2017. https://www.tekscan.com.
[43] Bendat JS, Piersol AG. Random data : analysis and measurement procedures. Wiley Series in Probability and Statistics; 2009.
[44] Caprani CC. A modal precise integration method for the calculation of footbridge vibration response. Computers and Structures 2013;128:116–27. doi:10.1016/j.compstruc.2013.06.006.
[45] Racic V, Brownjohn JMW. Mathematical modelling of random narrow band lateral excitation of footbridges due to pedestrians walking. Computers & Structures 2012;90:116–30. doi:10.1016/j.compstruc.2011.10.002.
[46] Kerr SC. Human Induced Loading on Staircases. 1998. doi:10.1016/S0141-0296(00)00020-1.
[47] Bocian M, Macdonald JHG, Burn JF. Biomechanically inspired modeling of pedestrian-induced vertical self-excited forces. Journal of Bridge Engineering 2013;18:1336–46. doi:10.1061/(ASCE)BE.1943-5592.0000490.
[48] Shahabpoor E, Pavic A, Racic V, Zivanovic S. Effect of group walking traffic on dynamic properties of pedestrian structures. Journal of Sound and Vibration 2017;387:207–25. doi:10.1016/j.jsv.2016.10.017.
[49] Živanović S, Johnson RP, Dang H V., Dobrić J. Design and construction of a very lively bridge. In:Topics in Dynamics of Civil Structures, Volume 4. Conference Proceedings of the Society for Experimental Mechanics Series., Springer, New York, NY; 2013, p. 371–80. doi:10.1007/978-1-4614-6555-3_41.
[50] Johnson O. Information theory and the central limit theorem. Imperial College Press;

2004.
[51] Chen SX. Probability density function estimation using gamma kernels. Annals of the Institute of Statistical Mathematics 2000;52:471–80. doi:10.1023/A:1004165218295.